AFOSR-TR- 81-0190

SEMIANNUAL TECHNICAL REPORT

(6)

A079982

No. 5

1 January 1980 to 30 June 1980

LEVEL II

AD A095851

Regional Seismic Wave Propagation

RONDOUT ASSOCIATES, INCORPORATED

P.O. Box 224

Stone Ridge, N.Y. 12484

DDC FILE COPY

Sponsored by

Advanced Research Projects Agency (DOD)

ARPA Order No. 3291-13

Monitored by AFOSR Under Contract # F49620-78-C-0043

Approved for public release; distribution unlimited.

81 2 27 126

UNCLASSIFIED

SECURITY CLASSIFICATION OF THIS PAGE (When Data Entered)

19 REPORT DOCUMENTATION PAGE		9 READ INSTRUCTIONS BEFORE COMPLETING FORM
1. REPORT NUMBER: 18 AFOSR-TR-81-0190	2. GOVT ACCESSION NO.: AD-A095851	3. RECIPIENT'S CATALOG NUMBER: Semiannual technical
4. TITLE (and Subtitle): 6 Regional Seismic Wave Propagation.		5. TYPE OF REPORT & PERIOD COVERED: rept. no. 5, INTERIM 1 Jan[redacted]-30 June[redacted]80
		6. PERFORMING ORG. REPORT NUMBER: 14 03-80-2
7. AUTHOR(s): 10 Thomas C. Chen [redacted] Paul W. Pomeroy		8. CONTRACT OR GRANT NUMBER(s): 15 F49620-78-C-0043, ARPA Order-3291
9. PERFORMING ORGANIZATION NAME AND ADDRESS: Rondout Associates, Incorporated, P.O. Box 224, Stone Ridge, NY 12484 — 12 60		10. PROGRAM ELEMENT, PROJECT, TASK AREA & WORK UNIT NUMBERS: 61102F 3291/30
11. CONTROLLING OFFICE NAME AND ADDRESS: AFOSR/NP, Bolling AFB, DC 20332		12. REPORT DATE: 11 31 Jul[redacted]80
		13. NUMBER OF PAGES: 58
14. MONITORING AGENCY NAME & ADDRESS (if different from Controlling Office): 16 3291 17 30		15. SECURITY CLASS. (of this report): Unclassified
		15a. DECLASSIFICATION DOWNGRADING SCHEDULE: NA

16. DISTRIBUTION STATEMENT (of this Report)

Approved for public release; distribution unlimited.

17. DISTRIBUTION STATEMENT (of the abstract entered in Block 20, if different from Report)

18. SUPPLEMENTARY NOTES

None

19. KEY WORDS (Continue on reverse side if necessary and identify by block number)

Seismic Discrimination
Regional Propagation-Comparative Study
Lg Wave-Review
Magnitude-Yield Relation
Yield-Related Parameters

20. ABSTRACT (Continue on reverse side if necessary and identify by block number)

In a review of studies on the seismic phase Lg, we describe its particle motion, dispersion, spectral content, mode of propagation, and magnitude-scale; we also tabulate the regional velocity, attenuation, and propagation efficiency for this seismic phase.

DD FORM 1 JAN 73 1473

UNCLASSIFIED

SECURITY CLASSIFICATION OF THIS PAGE (When Data Entered)

393833

The characteristics of Lg-wave propagation in the eastern United States are compared with those in different regions of the Soviet Union. Possible discriminants such as (i) Lg vs. P amplitudes, (ii) Lg/P amplitude ratios as a function of distance, and (iii) Lg energy ratios are found, similar to attenuation and group velocity, to be highly dependent on the propagation path. The valid application of these quantities to the problem of earthquake-explosion discrimination will therefore require regional studies more detailed than previously assumed.

A re-evaluation of the magnitude-yield relation and an examination of physical parameters which may be relevant to the estimated yield of underground nuclear explosions were performed. The preliminary results indicate that (i) the m_b vs. yield relation shows regional differences and dependence on the source medium, and (ii) the collapse volume and the diameter of the collapsed crater are usually proportional to the estimated yield.

ABSTRACT

In a review of studies on the seismic phase Lg, we describe its particle motion, dispersion, spectral content, mode of propagation, and magnitude-scale; we also tabulate the regional velocity, attenuation, and propagation efficiency for this seismic phase.

The characteristics of Lg-wave propagation in the eastern United States are compared with those in different regions of the Soviet Union. Possible discriminants such as (i) Lg vs. P amplitudes, (ii) Lg/P amplitude ratios as a function of distance, and (iii) Lg energy ratios are found, similar to attenuation and group velocity, to be highly dependent on the propagation path. The valid application of these quantities to the problem of earthquake-explosion discrimination will therefore require regional studies more detailed than previously assumed.

A re-evaluation of the magnitude-yield relation and an examination of physical parameters which may be relevant to the estimated yield of underground nuclear explosions were performed. The preliminary results indicate that (i) the m_b vs. yield relation shows regional differences and dependence on the source medium, and (ii) the collapse volume and the diameter of the collapsed crater are usually proportional to the estimated yield.

INTRODUCTION

The content of this report is divided into three topics: (i) a review of the available studies on the seismic phase Lg, (ii) a comparison of regional wave propagation in the US and the USSR, and (iii) a preliminary re-evaluation of the magnitude-yield relation and an examination of the physical parameters which may be relevant to the estimated yield of underground nuclear explosions.

Beginning with the current contract period, we will be reporting a series of reviews on (i) the seismic phases (Lg, Rg, Pg, Pn, Sn) that are potentially useful to the discrimination of explosions from earthquakes at regional distances, and (ii) the spectral characteristics of underground nuclear explosions. A lack of critical reviews on these crucial subjects has motivated us to undertake this ambitious project. We hope to achieve three goals through the reviews: (i) to compile and categorize the available observations into accessible format, (ii) to summarize the theoretical development in an overview fashion, and (iii) to emphasize the features that are related to the problems of earthquake-explosion discrimination. In this report, we will present a review on the seismic phase Lg. The review is subdivided into 7 topics: (A) particle motion and dispersion, (B) regional velocity, (C) spectral content, (D) wave guide and mode of propagation, (E) attenuation and propagation efficiency, (F) magnitude-scale based on Lg, and (G) others (Sn-to-Lg conversion, application to the earthquake-explosion discrimination problem, and search for oceanic Lg).

A comparative study of regional wave propagation in the eastern United States and different regions of the Soviet Union is presented in the second part of this Semi-Annual Technical Report. Five topics were selected to assess the feasibility of directly comparing the characteristics of regional seismic waves in the US and the USSR, and to evaluate their relative importance to the problem of earthquake-explosion discrimination. The topics are: (i) Lg vs. P amplitudes, (ii) Lg/P amplitude ratios as a function of distance, (iii) Lg group velocity, (iv) Lg energy ratios, and (v) Lg attenuation.

In studying regional seismic wave propagation, we often encounter the problem of how to calibrate a magnitude-yield relation at regional distances. This problem, although quite fundamental in nature, is by no means an easy one because a well-determined magnitude-yield relation requires a clear knowledge of (i) the source size, (ii) the amplitudes of seismic waves at different distances,

(iii) the effects of crustal structure at the source and the receiver, and (iv) the effects of the propagation path. The last part of this report re-examines this relation; it also describes the preliminary results from analyses of several physical parameters that are related to the yield of underground nuclear explosions.

I. Review of Lg

The purpose of this review is threefold: (i) to provide a summary of the available observations on Lg, (ii) to present the theoretical developments in an overview fashion, and (iii) to clarify or comment on what appears to us to be confusing concerning the interpretation of Lg.

The name Lg was assigned by Press and Ewing (1952) in their pioneering study on this seismic phase. "L" because the particle motion was predominantly of Love or transverse type, and "g" because the wave was believed to propagate in the granitic layer of the crust, and was therefore considered a surface-wave counterpart of the near-earthquake body waves Pg and Sg. These authors summarized the properties of Lg (for propagation paths in North America) succinctly in the abstract of their 1952 paper:

"Surface shear waves (Lg) with initial period 1/2 to 6 seconds with sharp commencements and amplitudes larger than any conventional phase have been recorded for continental paths at distances up to 6000 km. These waves have a group velocity of 3.51 ± 0.07 km/sec. and for distances greater than 20^0 they have reverse dispersion. For distances less than about 10^0 the periods shorten and Lg merges into the recognized near-earthquake phase Sg."

This and later investigations of Lg also point out that (i) the wave is not observed after approximately 100 km of propagation in the oceanic crust, (ii) the particle motion may contain a substantial amount of longitudinal and vertical components, and (iii) the observations may be explained by a collection of Airy phases of higher mode Love and Rayleigh waves.

The terms of Sg and Lg were used to refer to different waves in some earlier studies. Although both terms referred to high-frequency shear waves in the continental crust, the distinctions were based on differences in the observed frequency content, the distances of observation, and the interpretation in their mode of propagation. Sg, which is analogous to its compressional-wave counterpart Pg, referred to the direct shear arrival at short epicenter distances; while Lg referred to the superposition of normal modes, with frequencies slightly lower than those of Sg, at epicentral distances greater than about 10^0 (Press and Ewing, 1952). [There has been considerable confusion concerning the definitions of Pg and Sg. These terms replaced the $\overline{P}$ and $\overline{S}$ of Mohorovičić (1914) for

typographical convenience (pg. 86 of Jeffreys, 1976) and the supposed association with the granitic layer of the crust. While the definition of $\overline{P}$ referred to the direct compressional arrival at short distances with a velocity of about 5.5 km/sec (cf. Fig. 18-1 of Richter, 1958), the original data was obtained at distances over 150 km. Explosion data from California indicated that direct compressional arrivals at 120 km within the epicenter had a velocity near 6.34 km/sec. The Californian researchers consequently suggested the notation "p" for the direct wave at short distances and "$\overline{P}$" for the compressional wave with a velocity around 5.5 km/sec (p. 286-287 of Richter, 1958). The consensus at the present seems to be the use of the nomenclature P for direct compressional waves and the terms "Pn" and "Pg" for occasions when two distinct arrivals with velocities around 8.0-8.4 km/sec and 5.4-5.7 km/sec are observed.] In view of the consensus on the terminology of P-, Pg-, and Pn- waves and the arbitrary distinction between Sg and Lg, we are in favor of calling the direct shear arrival "S" and reserving the term "Lg" for shear waves with group velocities around 3.5 km/sec at epicentral distances where Sn (or the mantle-refracted S) becomes the first shear arrival. In this report, the term "Lg" will refer to both the "Lg" and the "Sg" cited in earlier seismological literature. In the following sections, we will attempt to summarize and discuss previous studies on the observations and interpretations of the Lg phase. We have divided the literature available to us into 7 topics: (A) particle motion and dispersion, (B) regional velocity, (C) spectral content, (D) wave guide and mode of excitation, (E) attenuation and propagation efficiency, (F) magnitude-scale based on Lg, and (G) others.

(A) Particle motion and dispersion.

Press and Ewing (1952) describe the particle motion of Lg in the following words:

"...During the first cycles the waves have approximately equal amplitudes on all three components, but the transverse horizontal rapidly gains amplitude and becomes several times larger than the other two within about 30 seconds. Approximately 1 minute after the commencement of the phase, the amplitude on the transverse component, having reached a value many times larger than that of S

or SS on any component, begins to decrease gradually, but does not drop to a value comparable with that of SS until about 30 minutes later, the period then being of the order 10-14 seconds. The group velocity for the latter part of this phase is certainly less than about 2 km/sec, the lower limit being uncertain ...". As for Eurasian events recorded at Uppsala and Kiruna, Båth (1954) reports that the particle motion of Lg was primarily transverse and was often observed at two different group velocity windows: Lg_1, at 3.54 ± 0.06 km/sec and Lg_2 at 3.37 ± 0.04 km/sec. Lehmann (1953) states that there was "considerable" vertical motion involved. All the authors mentioned above agreed that both the horizontal and the vertical components of particle motion were present in the Lg phase. Herrin and Richmond (1960) used a ray-approach analysis to explain the particle motion of Lg. Their calculations indicate that a strong SV type motion (i.e. with longitudinal and vertical components of motion) would be present with the SH-type motic initially; but during the later part of the wave train where the angle of incidence for the rays presumably becomes less steep, energy leakage to the bottom layers due to SV-to-P conversion would occur and the SV-motion tends to decrease faster than that of the SH-motion. The results of this analysis are in agreement with the observations of Oliver et al. (1955), but do not agree with their own observations at Dallas for earthquakes in southwestern United States and Mexico where strong SV-motion continued throughout the Lg wave-train. Herrin and Richmond also estimated the partitioning of energy between SV and P waves at different angles of incidence; Herrin (1961) pointed out some errors in their partitioning of energy and corrected them. By correlating the vertical component to the longitudinal component of the Lg particle motion, Sutton et al. (1967) found out that the particle motion of Lg from underground nuclear explosions and small earthquakes tended to be either transverse or mixed.

Aside from the qualitative comparison of Press and Ewing between the vertical and horizontal components of displacement, there are several other reports on their relative amplitudes. For the Lg amplitudes generated by the nuclear explosion GNOME in a salt mine of New Mexico, Romney et al. (1962) note that the displacements on all three components were approximately equal. But for earthquakes in the northeastern U.S. - southeastern Canada regions recorded at North American stations, Street (1976) reports that the maximum sustained horizontal component of Lg

consistently exceeded the vertical component by a factor of 3. For all epicentral distances in Iran, the resultant horizontal motion of Lg at 1 sec was usually twice that of the vertical component (Nuttli, 1980a). Båth (1956), however, found some Lg waves with no vertical particle motion at all.

Although Press and Ewing (1952) suggested the possibility of using higher mode surface waves to interpret the Lg phase, Oliver and Ewing (1957) were the first to calcualte the dispersion curves of higher mode Rayleigh waves and use them to explain the longitudinal and vertical components of Lg particle motion. In a later paper, Oliver and Ewing (1958) computed the dispersion curves from simple earth models for higher mode Love and Rayleigh waves and found that the M_2-mode (1st shear mode) and the second Love mode had similar velocities at the same period, which may explain the simultaneous arrivals of the vertical, longitudinal, and transverse components of ground motion for Lg. Dispersion curves and particle motions of higher mode Love and Rayleigh waves were computed for realistic earth models by Brune and Dorman (1963), and later including the effects of sphericity into the earth models by Kovach and Anderson (1964). Brune and Dorman also computed synthetic seismograms for the transverse component of Lg. The results of these authors confirm the hypothesis of Oliver and Ewing. Knopoff et al. (1973) presented further evidence to identify the transverse component of Lg motion as higher mode Love waves by (i) computing the relative spectral excitations for double-couple sources at different depths, and (ii), constructing synthetic seismograms for the higher mode Rayleigh waves and identified them as the longitudinal and vertical components of Lg motion.

The particle motion of the 1st shear mode (M_2) was computed by Oliver and Ewing (1957) to be retrograde elliptical; the same authors later reported that observations from an Arctic event (5/25/1950, 8:34:32; 65.5°N, 151.5°W) recorded at Palisades, confirmed their previous theoretical results on the particle motion (Oliver and Ewing, 1958). Barley (1978) traced the particle motion of higher mode Rayleigh waves (2.0sec $\leq$ T $\leq$ 3.5sec) for the group velocity window 3.0 to 3.5 km/sec, and found it to be retrograde elliptical. This result was predicted by the theoretical calculations of Panza et al. (1972) for the first three higher Rayleigh modes; these authors also found that at a given period the ellipticity

(defined as the ratio of the longitudinal component of particle motion to the vertical component) increased with decreasing mode number. For a shield structure with a low velocity channel (LVC) in the upper mantle, they found that at periods less than 4 sec. the ellipticity for the third higher Rayleigh mode was greater or equal to 0.7, whereas the ellipticity for the fundamental and the first two higher Rayleigh modes was greater or equal to 1.0.

(B) Regional velocity.

Table I is a summary of Lg velocities which were published in journals and reports available to us. Whenever possible, we tried to include information pertaining to the measurements of the velocity, such as the location of the seismic events and recording stations, the type of instrument used to record the events (horizontal or vertical component, short or long period, etc.), and the period of the Lg waves at which the measurement was made. Although the majority of the references cited did not specify their method of measurement. we deduced from their figures that most reported velocities were measured at the initial stage of the coda when a visible change in wave frequency or amplitude could be observed, either on the long- or short-period instruments. The measurements of Pomeroy and Nowak (1978), however, were made at the amplitude maxima of the Lg coda which seemed to be more unstable. Differences in the method of measurement and the recording instrument may account for the apparent discrepancy between the various reports. While measurements at the beginning of the coda probably correspond to the Airy phase(s) of higher mode surface waves with the fastest group velocity, measurements at the amplitude maxima probably coincide with the group velocity window where several Airy phases overlap. Whereas the former is indicative of the average properties of the wave guide, the latter which tends to be slower than the former, is probably not only more diagnostic of the detailed structure of the wave guide but also informative concerning the relative excitation of the various modes at the source (Knopoff et al., 1974). We would like to explore this possible aspect of Lg in a future study.

(C) Spectral Content.

The only sources known to us on the spectral content of Lg are derived from Street et al. (1976) and the Soviet seismological literatures (e.g. Antonova et al., 1978; Nurmagambetov, 1974). The studies on Lg propagation in the USSR were compiled and summarized in a report by Shishkevish (1979).

Street et al. derived their data from over 300 short-period, vertical component recordings of 78 earthquakes in the central U.S. In the period range they analyzed (approximately 0.05 - 10 sec.), the amplitude spectra generally indicate a falloff of ω^{-2} between the flat portions at the long- and short- period ends. Their spectra were corrected for the effects of instrument response, but not for the anelastic attenuation of the path.

The frequncy selection seismograph stations (ChISS) of the USSR have enabled the spectral analysis of Lg to become a routine procedure. Their results, commonly plotted as log (A/T) vs. log (1/T), generally display peaks at short epicentral distances. The peak is shifted towards lower frequencies as epicentral distance increases. This dependency of spectral peak on epicentral distance is also a function of propagation path. In these studies, the frequency ranged from 0.3 to approximately 20 Hz while the epicentral distance spanned from 30 to 3000 km. The falloff in their velocity amplitude spectra (i.e. displacement amplitude spectra multiplied by frequency) is also dependent on epicentral distances: at epicentral distances around 350 km, the falloff ranges from slightly greater than one to approximately two; whereas at epicentral distances greater than about 1000 km, the falloff remains less than 3. Since these measurements of Lg spectral content did not take the effects of geometrical spreading and anelastic attenuation into account, the spectral characteristics measured at short epicentral distances were probably more representative of the source spectra and a spectral falloff of about 2 could be taken as representative of the source falloff for the displacement amplitude spectra of Lg waves. The high-frequency spectral peaks observed in the USSR is probably an artifact of the velocity spectra plot; that is, the spectral peak will disappear if the plot is converted into a displacement amplitude spectra.

(D) Wave guide and mode of excitation.

Press and Ewing (1952) are, again, the first ones to point out that "... Lg is a wave which is confined to a surface or near-surface layer by wave-guide action..." based on the observed velocity and large amplitudes. Subsequent theoretical studies tend to support their claim although this conclusion is not reached without its share of confusion. In a study of Lg waves in Eurasia, Båth (1954) observed a correlation between hypocentral depth and the energies contained in Lg_1 and Lg_2. That is, the energy of Lg_1 generally decreased with increasing hypocentral depth, whereas the energy for Lg_2 reached a maximum when the source depth was around 45 km. He attributes the difference in energy distribution to several crustal channels or layers which transmitted waves at different group velocities. This claim, although sound when interpreted in terms of Airy phases with different group velocities, led to two unexpected results when viewed from the perspective of channel waves. Firstly, terminologies for waves which supposedly propagated in different channels of the crust and upper mantle proliferated (e.g. Båth, 1958). Secondly, several low-velocity channels in the crust and upper mantle came to be used as explanations for the efficient propagation of the various channel waves (Gutenberg, 1955; Båth, 1956, 1958).

Based on the dispersion curves of higher mode Love and Rayleigh waves, Oliver and Ewing (1957, 1958), Brune and Dorman (1963), and Kovach and Anderson (1964) found it possible to explain the frequency content and the group velocity of Lg waves by using the Airy phases of the higher modes. Kovach and Anderson (1964) also point out that the modes observed "...depend on the period range being studied and the depth of the source..." and that variations in the velocity and period of the observed Lg depended on the positions of the Airy phase, which in turn depended on the elastic parameters of the propagation path. If the interpretation of Lg waves as superpositions of higher mode surface waves is correct, then we would expect an additional dependence on the source radiation pattern. At periods greater or equal to 5 sec., radiation patterns of the first higher Love and Rayleigh modes compare favorably with calculated results (Mitchell, 1973 a,b). The observations of Sutton et al. (1967) on short-period (0.5-2.0 sec) Lg waves, however, indicate that "...

there seems to be no systematic difference in the short-period energy radiation pattern between the underground nuclear explosions and the earthquakes ..." and that the pattern of the energy-contours (or contours based on the maximum amplitude) could be better explained by a correlation with the major tectonic provinces of the United States. Since the modal composition of Lg at short periods is a combination of many higher modes, the observed amplitudes may not be diagnostic of the radiation pattern of the individual modes. Also, scattering is probably more important for short-period waves and its effects more likely to mask any azimuthal pattern that may be present.

Panza et al. (1972) showed that the collection of higher mode Rayleigh waves could be separated into a family of crustal waves and a family of channel waves in a structure containing even a slight low-velocity channel (LVC) in the upper mantle. As it is implied by the name, channel waves have most of the energy in the LVC and have essentially zero energy at the surface. Crustal waves, on the other hand, have most of their energy in the crust; consequently, only the fundamental mode and the crustal waves need to be considered for the excitation of Rayleigh waves. Knopoff et al. (1973) demonstrated that higher mode Love waves could similarly be divided into crustal waves and channel waves. For a structure without any LVC, the whole suite of higher mode Love and Rayleigh waves has to be taken into account for the ground motion of the Lg waves.

Knopoff et al. (1974) further establish that the group velocity and the periods of the Lg stationary phase could be diagnostic for the crustal thickness and the shear velocity in the crust and the upper mantle. In general, as the crustal thickness increased, both the group velocity of the late-arriving Lg stationary phases, U_{min}, and the period at U_{min}, T_{min}, tended to increase. Increasing the crustal velocity while keeping all other parameters constant would tend to decrease T_{min}, but increase U_{min}, the magnitude of Lg-excitation, and the general period-content of the Lg waves. These authors also demonstrate that (i) for thicknesses of the upper mantle lid greater than 20-25 km, Lg is insensitive to changes

in its thickness, and (ii) Lg is insensitive to the velocity in the upper mantle LVC. Panza and Calcagnile (1975) point out that higher mode contribution becomes more significant as the period decreases and/or as the hypocentral depth decreases.

As for the low-velocity channel in the crust and/or upper mantle, Oliver and Ewing (1958) concluded that it was not necessary to explain the characteristics of the Lg phase. Knopoff et al. (1973) and Panza and Calcagnile (1975), based on more modes extending to shorter periods, reached the same conclusion concerning the Love- and Rayleigh-type motions of the Lg phase, respectively.

Most of the investigators mentioned in this section would probably maintain that the characteristics of Lg can be explained by the anelastic attenuation of the crust-mantle layers, the frequency response of the seismograph system, and the superposition of higher mode surface waves. Ruzaikin et al. (1977), on the other hand, state that they "...remain unconvinced that normal modes will allow useful interpretation of Lg when more detailed data on its structure are obtained ..." and suggest that lateral heterogeneity had a key role in shaping the characteristics of the observed Lg. Their argument was based on the discrepancy between calculations from higher mode surface waves which predicted the duration of Lg to be confined in the group velocity windows of approximately 3.5-3.1 km/sec, and observations of the Lg phase which indicated that its amplitude was significant in the group velocity window 3.5 - 2.8 km/sec. Oceanic Rayleigh waves of the fundamental mode ($T \geq 12$ sec) also exhibit similar "stretching" in duration. These waves have nevertheless been instrumental in shaping our present understanding concerning the oceanic structure. Thus, while we share the belief with Ruzaikin et al. that heterogeneties in the propagation path are important in shaping the waveform of Lg, we also believe that the normal mode theory, when supplemented with theories or methods which can take heterogeneity in the path into consideration (e.g. the scattering theory of Aki, 1969), will serve to improve the explanation for the Lg phase.

(E) Attenuation and propagation efficiency.

This section deals with the measurement of amplitude-diminution as a function of epicentral distance; the title of the section reflects, respectively, the quantitative and qualitative aspects of it. The former refers to the rate of anelastic absorption of the wave's kinetic energy per unit distance, while the latter provides a descriptive measure for the efficiency of the medium in transmitting Lg waves.

In seismological literature, attenuation is usually measured in terms of the attenuation coefficient, γ , or the attenuation quality factor, Q . These two quantities can be related via the following equation:

$$\gamma = \frac{\pi f}{Q u} \qquad (1)$$

where f and u are the frequency and the velocity of the wave, respectively. For Lg waves, measurements of γ and Q , compiled in Table II, have been obtained by three approaches: (i) time-domain, (ii) frequency-domain, and (iii) coda.

The time domain approach entails three steps: (i) measure the wave amplitude at different epicentral distances, (ii) correct the amplitudes for the effect of geometrical spreading, and (iii) estimate the γ or Q that would explain the falloff of the amplitude in relation to distance. Nuttli (1975, 1978, 1980 a, b) and Street (1976) chose to combine steps (iii) and (ii) together, and compared the observed amplitudes directly with curves that include the effects of geometrical spreading and different degrees of attenuation. The frequency-domain approach has the advantage of being able to take the source radiation pattern into account. The procedure used by Mitchell and coworkers, who have been the primary advocates of this approach on higher mode surface waves, is similar to that employed for the study of the fundamental mode (Tsai and Aki, 1969). Again, three steps are involved in this procedure: (i) determine the amplitude apectra for the fundamental and higher mode surface waves by applying a frequency-velocity filter (e.g. the multiple-filter technique

of Dziewonski et al., 1969), (ii) estimate a fault-plane solution from body- and/or surface-wave data, and (iii) calculate the attenuation coefficient that would produce the best fit between the observed amplitudes and the radiation pattern computed at each period. To date, this approach has been limited to the analysis of the fundamental and the 1st higher mode (Mitchell, 1973 a,b; Cheng and Mitchell, 1980). The coda approach, which was derived from the scattering theory of surface waves (Aki, 1969), has been applied successfully to data from narrow-band seismographs to establish (i) scaling laws for local earthquakes, and (ii) estimates of regional Q (Aki and Chouet, 1975; Chouet et.al., 1978; Rautian and Khalturin, 1978). Herrmann and co-workers recently modified this method for data derived from broadband seismographs. They estimated the regional Q from Lg waves by measuring (i) the predominant frequency in the coda as a function of time, and (ii) the coda shape (Herrmann, 1980, Singh and Herrmann, 1979).

The propagation efficiency of a region is usually estimated by measuring the frequency content and wave amplitude (usually in relation to the level of the ambient noise or the amplitude of another phase); in general, three terms: clear, weak, and none, are used to describe the amplitude of the Lg phase. "Clear" usually refers to an impulsive, large-amplitude, high-frequency arrival; "weak" refers to a drawn-out, small, low-frequency arrival; and "none" is indicative of completely inefficient Lg propagation. Although different authors have set their standards for clear and weak Lg somewhat differently, their conclusions concerning the propagation efficiency of a given region are, surprisingly, quite uniform. A list of regional studies on the propagation efficiency of Lg is compiled in Table III.

In interpreting the inefficient propagation of Lg in the Tibetan plateau, Ruzaikin, et al. (1977) proposed two explanations which are probably applicable to most areas with major tectonic boundaries. Firstly, a disruption, termination, or vertical displacement of wave guide (which is either the entire crust or part of it) will seriously affect the propagation efficiency of Lg waves; secondly, high attenuation in the crust will also be able to affect the ability to transmit Lg. The ocean-continent boundary is probably a disruption or termination of the wave guide for Lg; disap-

pearance of Lg waves after crossing approximately 100 km of oceanic structure is a well documented observation (e.g. Press and Ewing, 1952; Båth, 1954; etc.). This peculiar property of Lg waves to propagate only in the continental crust was used by Oliver et al. (1955) to map the continental structure in the Arctic regions.

Båth (1956) and Gutenberg (1955) report that the Lg phase was weakened or disappeared when crossing recent mountain chains. Shishkevish (1979), in his compilation of studies on Lg propagation in the Soviet Union, also notes that the Lg phase was attenuated when crossing Tien Shan, Pamir-Hindu Kush, and the Himalayas. He also points out that "...the propagation of Lg across the Tien Shan is less efficient when paths are more oblique to the trend of the range than when they are perpendicular to it ...". Uniformity of the structure (Chinn et al., 1980) and the complexity of geology (Street, 1976) in the propagation path are also considered important in determining the attenuation of the Lg amplitude. In summary, the presence of a uniform, high-Q wave guide is essential for the efficient propagation of Lg; in the case of a non-uniform or low-Q wave guide, the degree of non-uniformity of the wave guide and the length of propagation in it are both important in determining the fraction of Lg-energy that will be observed.

(F) Magnitude-scale based on Lg.

Since Lg is often found to be the largest phase at regional distances, it is natural that a magnitude-scale based on Lg amplitude would become important to studies on regional seimsicity. Based on LRSM reports from 78 underground nuclear explosions, Baker (1970) proposed a general formula of the form,

$$M_{Lg} = \log_{10}(A/T) + Q(T, \Delta) + S(T) \qquad (2)$$

to calculate the magnitude-scale from Lg amplitudes. $Q(T, \Delta)$ represents a correction term for the attenuation, and $S(T)$ is a term for station correction. Baker obtained an expression for $Q(T, \Delta)$, as a sixth degree polynomial of

distance, by minimizing the difference between $\log_{10}(A/T)$ and the reported m_b for each event; he also assigned tentative corrections for each station. M_{Lg} calculated by Baker indicates less scatter than the reported m_b.

Nuttli (1973) formulated a magnitude scale for Lg while studying its attenuation in the eastern United States. He assumed that the term $Q(T,\Delta)$ in equation (2) has the form $C(T,\Delta)\ \log_{10}\Delta$, and subsequently found two magnitude formulae, applicable at different distance ranges, for 1-sec Lg of "sustained" (3 or more cycles) amplitudes.

$$M_{Lg} = 3.75 + 0.9 \log_{10}\Delta + \log_{10}(A/T) \qquad 0.5^{0} \leq \Delta \leq 4^{0}$$
$$= 3.30 + 1.66 \log_{10}\Delta + \log_{10}(A/T) \qquad 4^{0} \leq \Delta \leq 30^{0}$$

Street (1976) and Bollinger (1979), respectively, found Nuttli's formulae to be applicable in northeastern and southeastern North America, provided that the maximum distance is limited to approximately 2000 km.

Street et al. (1976), on the other hand, assumed $C(T,\Delta)$ to be known and then specified $S(T)$ such that the magnitude scales at different periods were set equal for an $m_b = 1.5$ event. For an $m_b = 2.5$ event, the magnitude calculated at 0.1 sec. according to their formulation would be 1.8, and the discrepancy between m_b and $m_{0.1}$ increased rapidly with increasing m_b. Since there is no implicit or explicit reasoning behind the assumption of a known $C(T,\Delta)$, we are inclined towards the procedure of determining $C(T,\Delta)$ experimentally and then calculating the $S(T)$ so that a uniform magnitude would be obtained at all periods.

(G) Others.

Sn to Lg conversion appears to occur near the margin of the American continents. For events from the West Indies and Mexico recorded at North American stations, Isacks and Stephens (1975) identified the prominent phases which arrived after Sn as possibly a converted Lg at the continental margin. Chinn et al. (1980) observed similar conversions for events in the Nazca Plate recorded at South American stations. In neither of the studies was any Lg to Sn conversion observed.

A number of investigators have explored the possibility of using the ratio of Lg-amplitude to P-amplitude as a discriminant for the earthquake and the underground explosion populations. This possibility was tested by Pomeroy and Nowak (1979), Pomeroy (1980), Nuttli (1980 b), and Gupta et al. (1980) for propagation paths in western and central Soviet Union, and by Pomeroy and Nowak (1979) and Pomeroy (1980) for propagation paths in eastern and western United States, respectively. Their findings indicate a tendency for the Lg to P amplitude ratios to be greater than 1.0 for earthquakes and less than 1.0 for underground nuclear explosions. The ratios, however, appear to be strongly dependent on on the epicentral distance and the regional attenuation in the propagation paths and therefore cannot be used reliably as a discriminant between explosions and earthquakes.

Contrary to higher-mode surface waves in continental structures, higher-mode Love waves in sediment-covered oceanic structures do not form a coherent family of arrivals at short periods (Knopoff et al., 1979). This phenomenon can serve to explain the absence of Lg waves in the oceanic structure. These authors also point out that since a large fraction of the shear energy at the stationary phases of higher-mode Love waves is concentrated in the sedimentary layer, absorption by the low-rigidity sediment and scattering due to variations in its thickness can account for the rapid attenuation of the higher-mode Love waves in oceanic structures.

TABLE I - Lg Velocity

REGION	VELOCITY	STATION (Instrument)	EVENTS	COMMENTS	REFERENCE
Africa	3.48-3.60	WWSSN and temporary SP stations	Earthquakes in Africa	Velocity higher in SE than in N part	Gumper and Pomeroy (1970)
S. Africa, Transvaal	3.68				Willmore et al. (1956)
"	3.66	SP temporary stations			Gane et al. (1956)
Australia	3.50	Riverview (Wiechert, (Galitzin)	Earthquakes in central and western Australia	Initial period $\simeq$ 3-6 seconds.	Bolt (1957)
Australia	3.44±0.04		Explosions in Australia		Bolt et al. (1958)
Eurasia	3.54±0.06	Uppsala, Kiruna, Bergen (Wiechert)	Earthquakes in Eurasia	Lg_1	Båth (1954)
"	3.37±0.04			Lg_2	"
Mediterranean region	3.40±0.02			Sg	Jeffreys (1952)
N. America	3.51±0.07			Initial period $\simeq$ 0.5 - 6 sec.	Press and Ewing (1952)
N. America, Eastern	3.57				Lehmann (1953)
Canadian Shield	3.54				Hodgson, (1953)
"	3.60-3.70	Ottawa, Resolute, Palisades Halifax (LP and SP)			Brune and Dorman (1963)
"	3.56				Horner et al. (1973)
California	3.54±0.02	SP network in California	Earthquakes from N. Calif. and Nevada		Press (1956)
Sierra Nevada	3.53±0.02	"	"		"
Central Valley & Coastal Ranges	3.55±0.03	"	"		"
U.S., Central	3.49		Earthquakes in Tenn.		Nuttli (1956)
"	3.49-3.80			Summary of previous studies	McEvilly (1964)
"	3.03-3.39	WWSSN (SP)	SALMON explosion	Velocity measured at maximum amplitude of Lg coda	Pomeroy and Nowak (1978)
"	2.18-3.72	"	Earthquakes in eastern and central N. America		"
U.S., Eastern	3.19-3.35	WWSSN (SP)	SALMON explosion	"	"
"	3.04-3.80	"	Earthquakes in eastern and central N. America	"	"
U.S., Central and SE	3.65±0.04	Saint Louis Univ. network (Wood-Anderson torsion seismometer)	New Madrid earthquakes		Stauder and Bollinger (1963)
U.S., SE	3.50±0.13	WWSSN (SP)	Earthquakes in SE United States	T $\simeq$ 0.7±0.1 sec	Bollinger (1979)
	3.52±0.10	"		T $\simeq$ 0.8±0.1 sec Vertical comp.	

TABLE II - Lg Attenuation

REGION	γ (10^{-3} km^{-1})	Q	n (Δ^{-n})	STATION	EVENTS	COMMENTS	REFERENCE
Iran	4.5 3.0			WWSSN (MSH,SHI,TAB) "	Earthquakes in Iran	1 sec Lg 3 sec Lg	Nuttli (1980a) "
N. America, Eastern	0.63 .90			WWSSN, LRSM, CNS, SLU	Earthquakes in central US	1 sec Lg(Z) 3-13 sec Rayleigh	Nuttli (1973) "
N. America, Central and eastern	0.63 0.23 0.8			WWSSN, LRSM, CNS " "	Earthquakes in SE Missouri "	1 sec 1st shear 10 sec 1st shear 4-6 sec 1st Love	Mitchell (1973a) " Mitchell (1973b)
United States		450±30		LRSM	NTS explosions	Lg	Press (1964)
U.S., NE	0.99			WWSSN, LRSM, CNS	Earthquakes in NE North America	1 sec Lg(Z)	Street (1976)
U.S., Central and eastern	0.87±0.66	1456		WWSSN (BLA)	Earthquakes in E. and central U.S.	Lg-coda	Herrmann (1980)
U.S., Eastern	0.63			WWSSN, NEUSSN	SALMON explosion and N. American earthquakes	0.3-1.0 sec Lg(Z)	Pomeroy (1979)
U.S., SE	0.63 0.90			WWSSN, LRSM "	Earthquakes in SE U.S.	1-sec Lg(Z), 100-700 km " 700 km	Bollinger (1979)
New Madrid, N.C.	6.0	1500		WWSSN	Local Earthquakes	0.1-sec Lg	Nuttli (1978)
Mississippi Valley		1500-2000				0.1-1.0 sec Lg	Nuttli and Dwyer (1978)
U.S., SE	-2.9±6.4	2190		USGS (GRT, Tenn.)	Earthquakes in eastern U.S.	Lg-coda	Herrmann (1980)
U.S., Western	4.8±1.3 2.5±1.0	229 396		WWSSN (BKS) WWSSN (DUG)	Earthquakes in western U.S.	" "	" "
U.S, W & SW of Western U.S., NW of western Colorado plateau N. Rocky Mountains		130-180 180 300-330 600-700		WWSSN " " "	Earthquakes in western U.S. " "	Lg-coda " " "	Singh and Herrmann (1979) " " "
USSR, Central Asia " , Dzhungaria " , Altai and Sayan			≃ 2 "	Network from Pamir to Lena River	Earthquakes in central and SW Asia	Lg	Nersesov and Rautian (1964)
Tien Shan " of Lake Baykal "		250 500 1200				Lg 1 sec - Lg 0.3 sec - Lg	Shishkevish (1979) " "
Near Caspian Sea USSR, S. border	1.35 3.15			WWSSN "	Earthquakes and explosions in central and western USSR	1 sec Lg(Z) "	Nuttli (1980b) "
USSR, S. " "	1.5-2.0 4.5-5.5 2.5-4.0	450-600 160-200 225-360		WWSSN (MSH, NIL, KBL, QUE, TAB) " "	Earthquakes and explosions in USSR " "	Low topographical relief High topographical relief Mixed path Both vertical and horizontal component of Lg	Springer and Nuttli (1980) " "

TABLE III Propagation Efficiency

REGION	STATION (Instrument)	COMMENTS	REFERENCE
Eurasia	Uppsala, Kiruna, Bergen (Wiechert, Galitzin)		Båth (1954)
E. Europe and Asia		Compilation	Piwinskii and Springer (1978)
Eurasia, Central			Ruzaikin et al. (1977)
USSR, Central	WWSSN		Pomeroy (1979)
USSR, E and Central China, NW and Central		Compilation "	Shishkevish (1979) "
Middle East	WWSSN (EIL, IST QUE, SHI, TAB)		Kadinsky-Cade (1980)
U.S., E.	WWSSN, NEUSSN		Pomeroy (1979)
California			Gutenberg (1955)
U.S., SW and NE Mexico	Dallas		Herrin and Minton (1960)
S. America, W.	WWSSN		Chinn et al. (1980)

II. Contrast in Lg Wave Propagation in the Eastern United States with that in the USSR.

The purpose of this report is to portray and discuss similarities and differences in Lg wave propagation in the eastern United States with that in different portions of the USSR. The discussion will be divided into five areas:

1. Lg vs. P amplitudes
2. Lg/P amplitude ratios as a function of distance
3. Lg group velocity
4. Lg energy ratios
5. Lg attenuation

1. Lg vs. P amplitudes.

A plot of Lg vs. P wave amplitudes for earthquakes in the eastern United States is presented in Figure 1. The dashed line in this figure represents a wave amplitude of Lg approximately equal to 10 times the wave amplitude of P (Lg $\approx$ 10 P). Also shown in this figure are:

1. Amplitudes of Lg and P measured from records of the underground explosion SALMON shown by solid triangles.
2. A solid line (Lg $\approx$ 6.5 P) based on 104 measurements of Lg and P from earthquakes in Africa.

In general, this figure quantifies the general observation in the eastern United States that Lg is commonly the largest regional seismic wave recorded and often is the only signal recorded from small events.

In the USSR, the situation is complicated by the fact that most of the data available are from WWSSN or other recording stations located outside the USSR while the events of interest are within the USSR usually on the other side of significant tectonic boundaries. With that in mind, the data in Figure 2 can be explained. The few earthquake events in the western portion of the USSR shown as solid squares scatter around the solid line represented by Lg = P/10; that is, the amplitudes of Lg are smaller than amplitudes of P. The data from the Gazli earthquakes falls closer to the dashed line (Lg = P). For both data sets, the Lg amplitudes are significantly smaller than those observed in the eastern United States. When data published by Soviet authors for earthquakes in the eastern USSR is examined, the situation is significantly different as

shown in Figure 3. For earthquakes not crossing major tectonic boundaries (Events 1-12), Lg is the predominant phase on the seismogram. Thus, in this respect, the eastern portions of the US and the USSR are similar.

For explosions in the western central portions of the USSR, the data falls about or below the line Lg = P, indicating a similarity to the earthquake data. This is shown in Figure 4 for all the USSR explosions as studied by Rondout during this contract. This indicates little contrast with the earthquake population and suggests that the propagation path rather than the source properties exert a predominant effect on Lg propagation in this region. This result is in agreement with the SALMON results in the eastern United States.

2. Lg/P ratios as a function of distance.

Lg/P ratios have been suggested as a possible discriminant between explosion and earthquake sources. In Figure 5, data on the logarithm of the ratio $\frac{(A/T)\ Lg}{(A/T)\ P}$ are plotted vs. distance for all events studied by Rondout (with the exception of the eastern USSR events). The earthquakes in the eastern USSR would plot as positive values in this data. Two straight lines represent the best least-squares fit to the explosion and earthquake data. Although the data from earthquakes is sparse there does not appear to be a significant difference between the two populations. Because the data presented here comes from a wide variety of source-receiver patterns, more detailed comparisons of the two populations on a path-by-path basis are required.

Although similar data on explosion for the eastern United States is limited to that of SALMON, it can be inferred from a examination of Figure 1 that the explosion and earthquake data would fall in the same general region on a plot such as that of Figure 5.

3. Lg group velocity.

An initial observation that the Lg group velocity for the SALMON event was low led to a more extensive study of the group velocity values for Lg both in the eastern US and in the USSR. Data for a number of earthquakes in the eastern United States are presented in Figure 6 (WWSSN and LRSM data) and 7 (NEUSSN data). These show that the group velocity from a number of event-station pairs falls below the generally accepted 3.5 km/sec value. The solid traingles in Figure 6 represent data from the SALMON explosion. Possible explanations for these low group velocities include the following two hypotheses:

1. The propagation paths from SALMON in general contain a segment with a thick sequence of sediments in the Mississippi Embayment and this thick cover of low velocity material may significantly lower the average group velocity of Lg. This is partially substantiated by the low values of group velocity observed on other paths with smaller proportions of their patterns in the Embayment which exhibit low values of group velocity (still higher than SALMON, however).
2. Because SALMON is a shallow event, different relative mode exitation at the source compared to the deeper earthquakes will occur. The different mode excitations could result in the waves sampling of the near surface intervals giving rise to lower group velocities.

To investigate this possiblility further, data from earthquakes and explosions in the USSR was examined and the results are presented in Figure 8. The solid squares and the shaded region represent earthquake data while explosion data are represented by solid angles. Although much additional work remains to be done, these events are not encouraging for the use of Lg group velocity alone as a discriminant.

4. Lg Energy ratios.

To investigate the observed low group velocities for SALMON further and to quantify more fully differences in group velocity, an energy ratio method was devised. Basically, this is a ratio of the energy arriving in the group velocity window 4.0 to 3.4 km/sec to the energy arriving in the window 3.4 km/sec-2.8 km/sec. The results from this analysis indicate that SALMON has a relatively low ratio while earthquakes in the US have a higher value. The energy in each group velocity window was measured by measuring the area encompassed by the envelope of the wave train in a method similar to the AR method as used by Brune on longer period surface waves. The results of these measurements for SALMON and several eastern US earthquakes are presented in Figure 9. The separation between SALMON and the earthquakes is clear.

The results from a similar analysis on earthquakes and explosions in the USSR are presented in Figure 10. Although the earthquake data is again sparse, the populations seem to overlap and discriminations is not achieved. Current studies involving these ratios on a more local scale may provide greater understanding of discrimination capability.

5. Lg attenuation

Lg attenuation has been the subject of numerous investigations (see Part I of this report). 'Hard' data on attenuation, particularly comparable data from different regions, is still not readily available. As part of the regional wave propagation study by Rondout, attenuation measurement in the eastern US and in the Soviet Union were carried out and the results are presented in Figures 11 and 12 respectively. Figure 11 is a composite plot based primarily on eastern US earthquake data. Since the data is composited, it was normalized to a common magnitude. For comparison, Nuttli's approximation to $\gamma = 0.07\ \mathrm{deg}^{-1}$ is shown as a solid line and the best least square fit to the data is shown as the dashed line.

In Figure 12, Lg attenuation is plotted for USSR explosions. The explosion data was normalized through yields assigned by Dahlman and Israelson and thus is subject to even greater uncertainties than earthquake data. A straight line representing an amplitude fall-off of proportion and $1/\Delta^3$ is shown. Also shown in Figure 12 are four paths (indicated by crosses) within the USSR as derived by Soviet investigators.

Although a direct comparison of Figures 11 and 12 is difficult because of different scales, our tentative conclusion is that, on the average, the two data sets could be derived from the same population. Work by Nuttli and Springer indicates that portions of the USSR may have attenuations intermediate between those of the eastern and western US. Our composites would average out these differences.

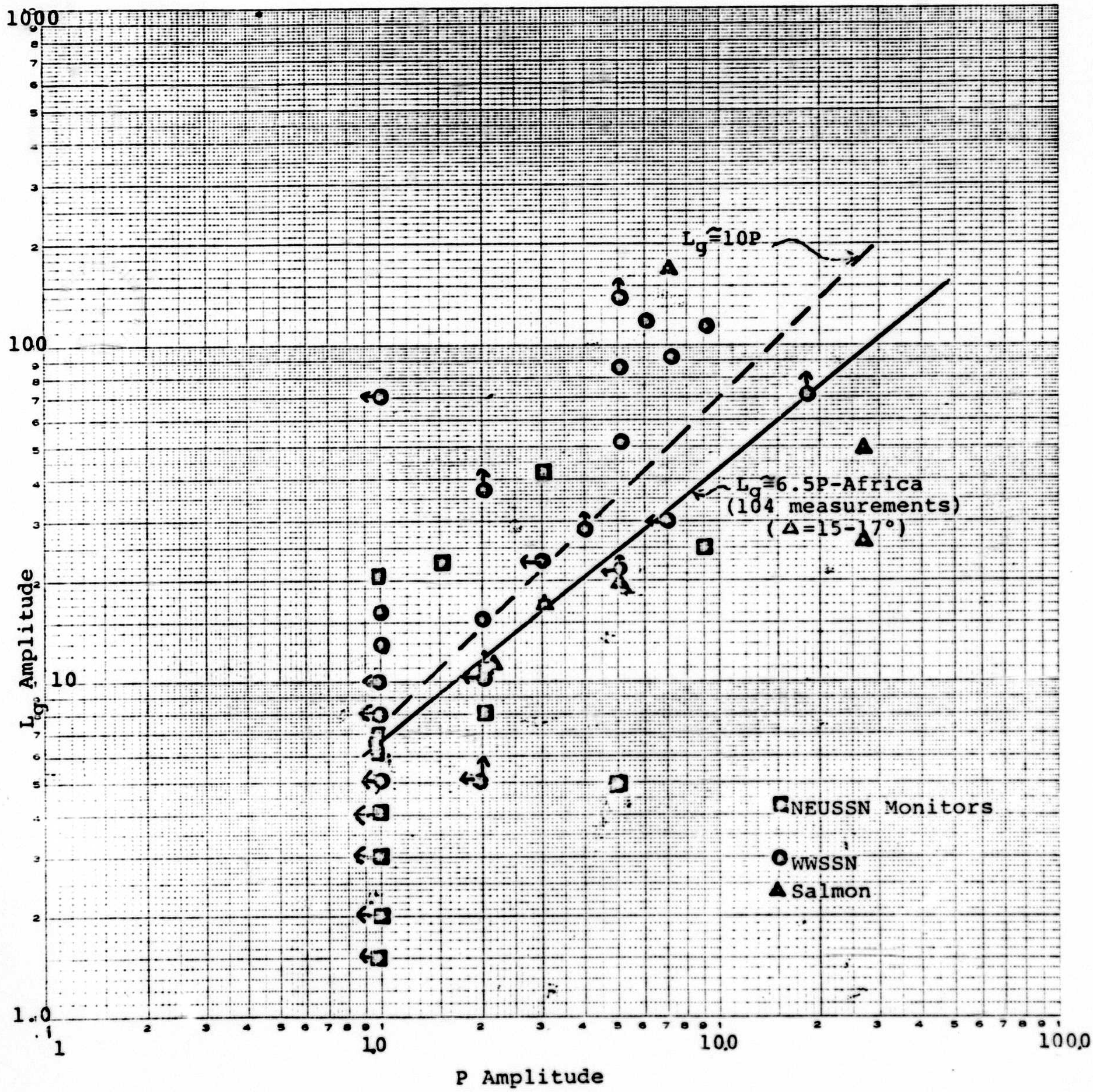

Figure 1. L_g amplitude vs. P wave amplitude

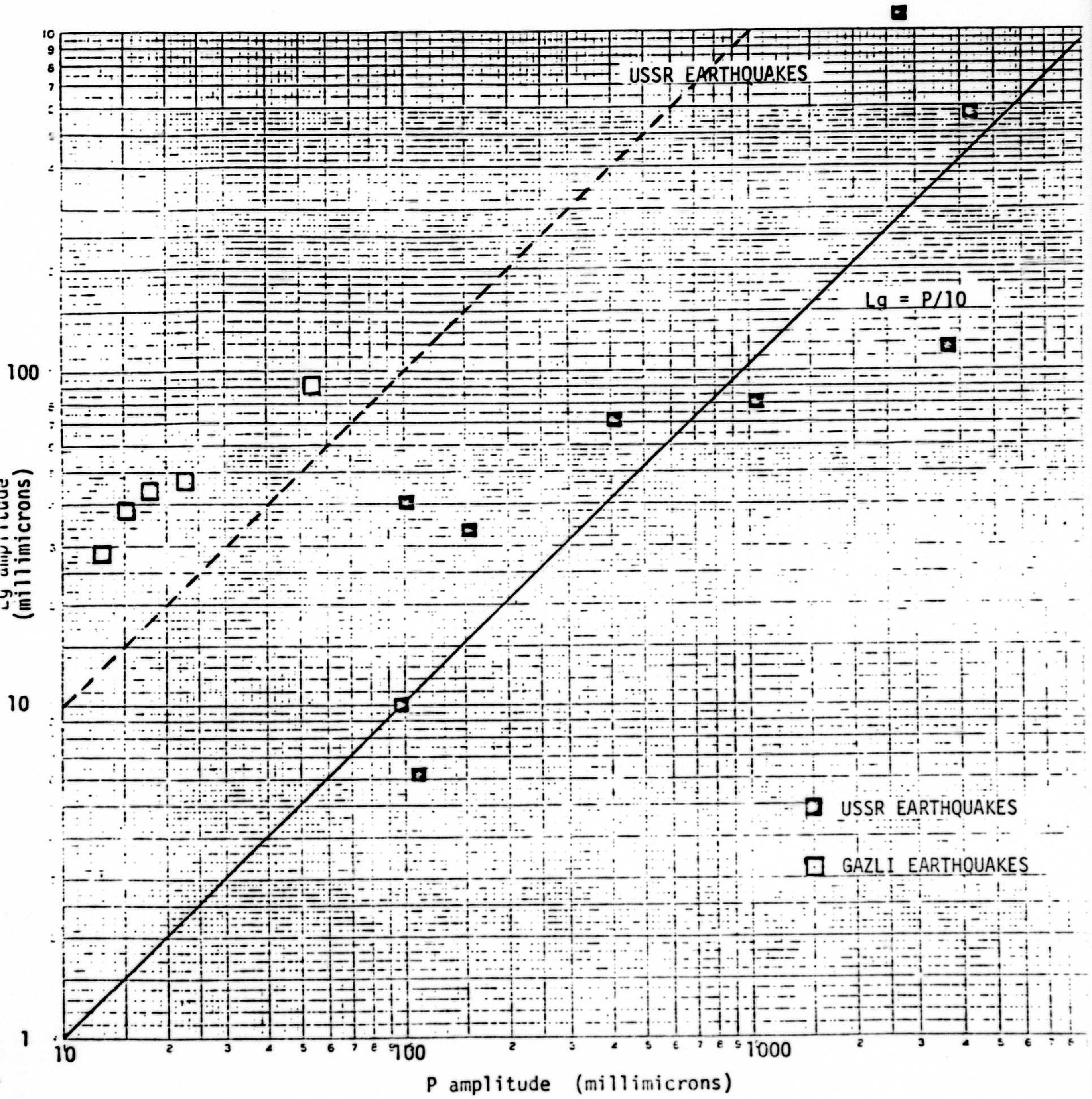

Figure 2. A Composite of the Earthquake Data from Earlier Studies Comparing Lg(Z) and P(Z) Amplitudes. Note that the equation of the solid line shown here is amplitude of Lg = Amplitude of P/10 and the equation of the dashed line is Amplitude of Lg = Amplitude of P.

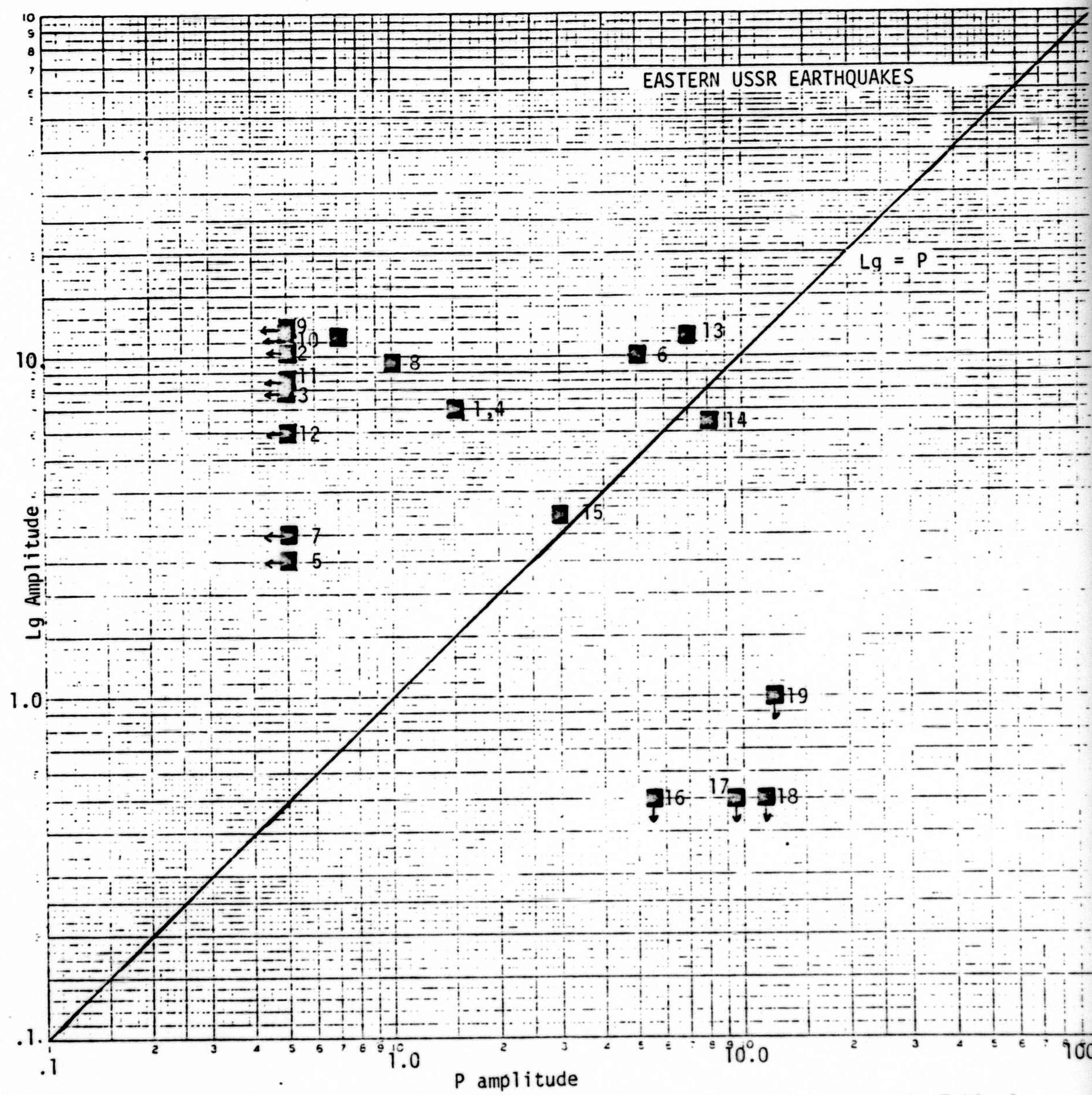

Figure 3. Lg amplitude vs. P amplitude for eastern USSR earthquakes listed in Table I. The equation of the line is Amplitude of Lg = Amplitude of P.

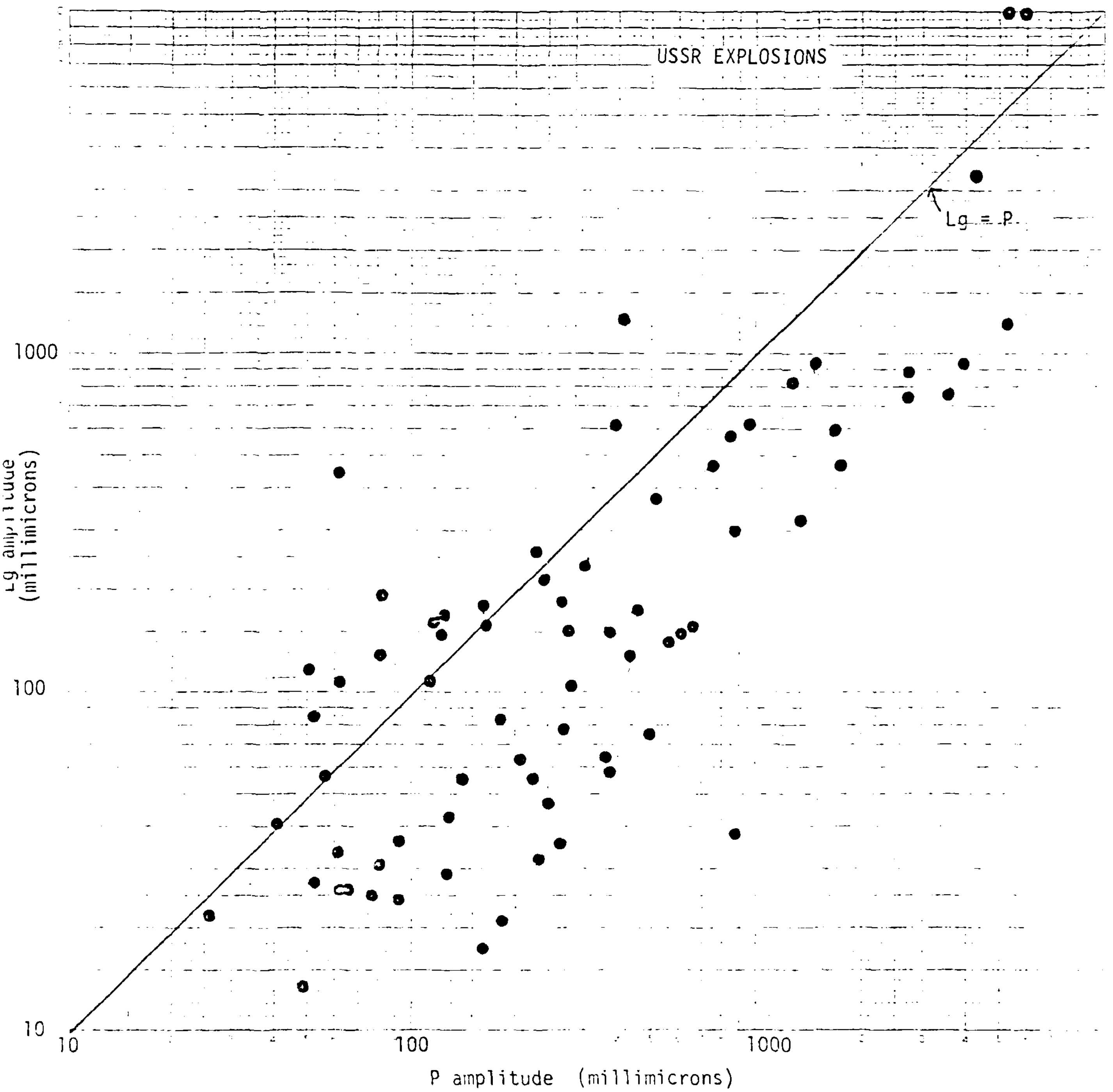

Figure 4. A Composite of Explosion Data from this and Earlier Studies of the USSR Comparing Lg(Z) and P(Z) Amplitudes.

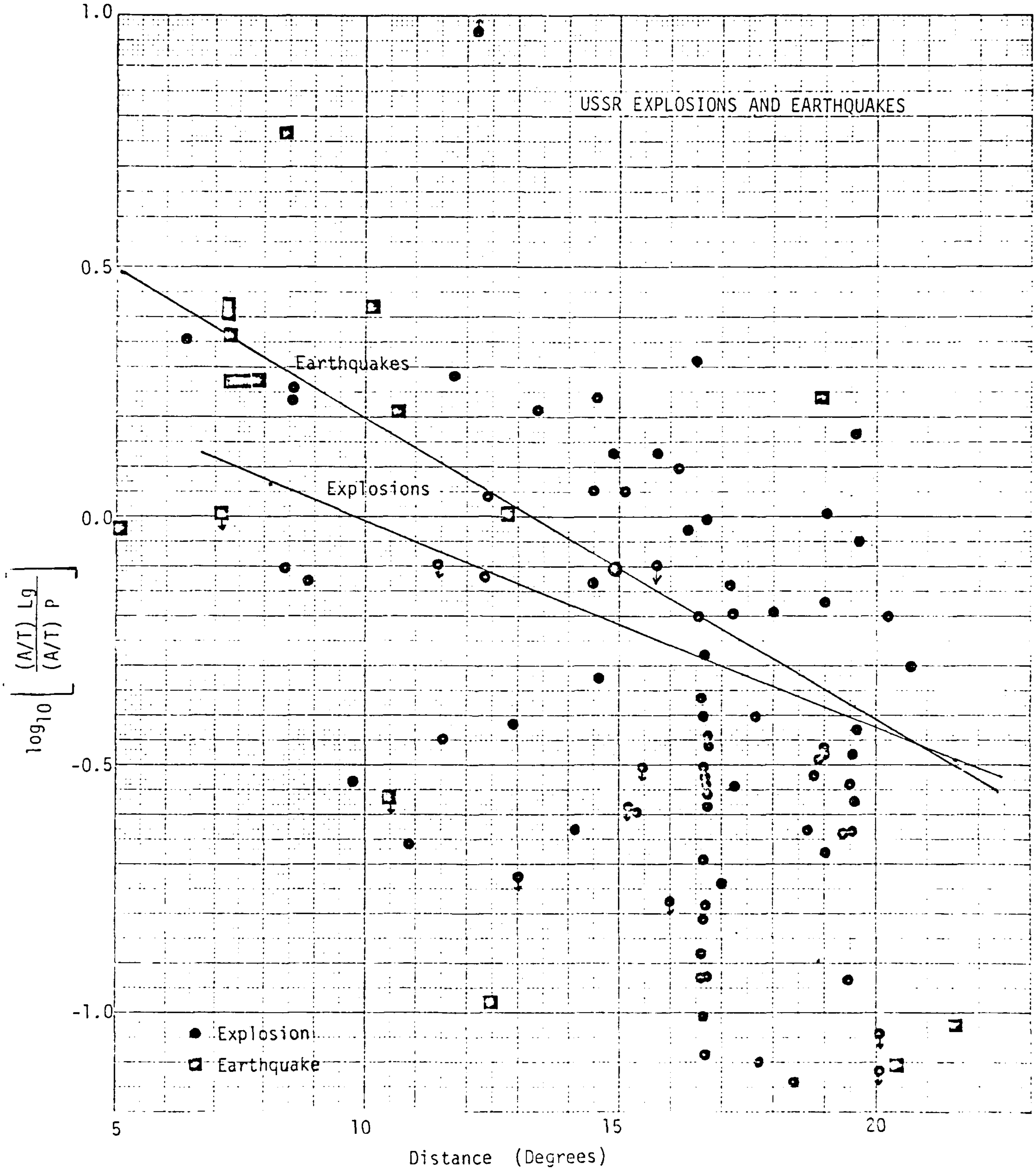

Figure 5. Composite Amplitude Ratios for all USSR Earthquakes and Explosions Analyzed to Date.

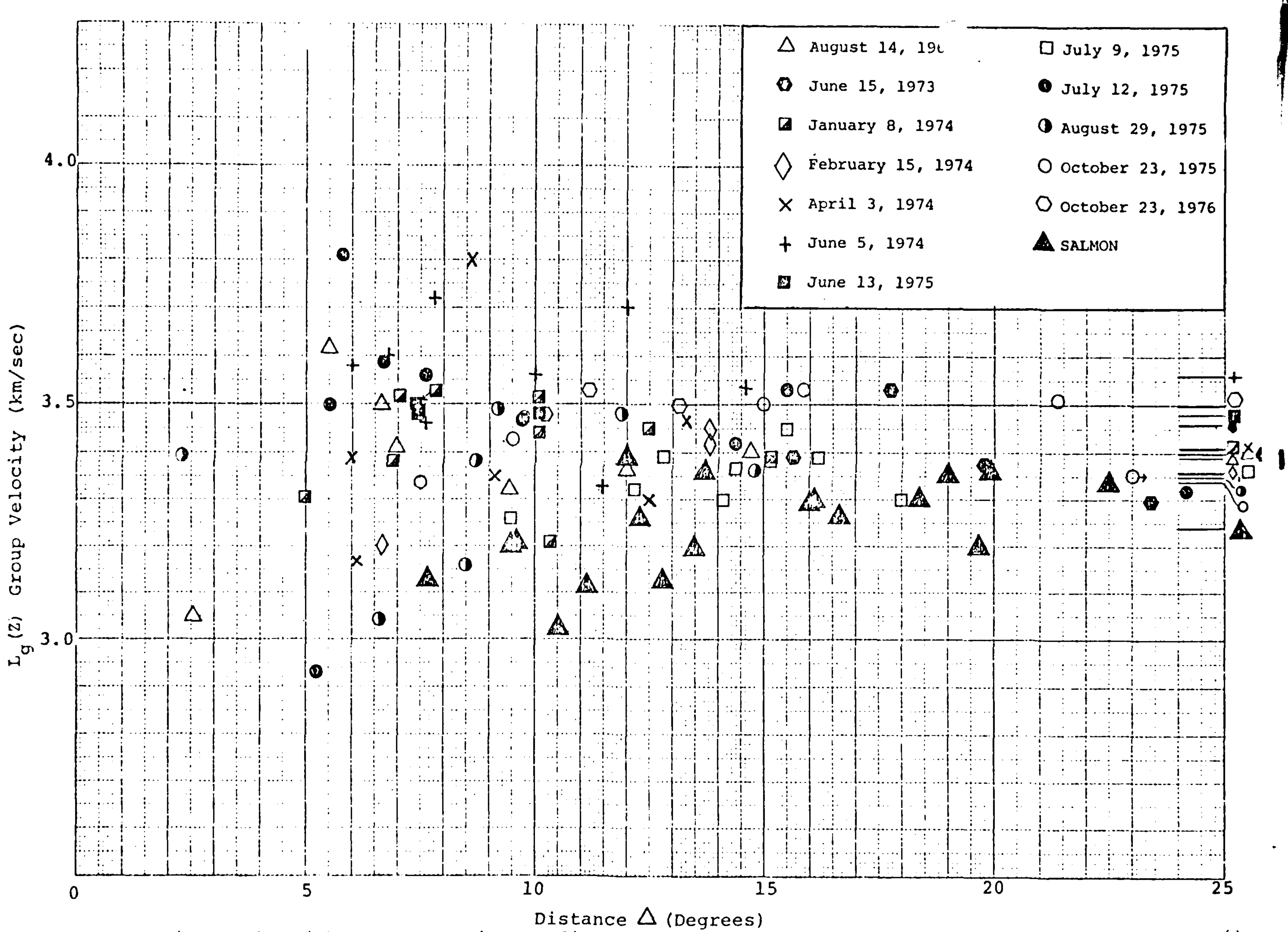

Figure 6. $L_g(Z)$ group velocity vs distance as determined from the WWSSN and LRSM data Bars on the right hand side represent averages determined for each set.

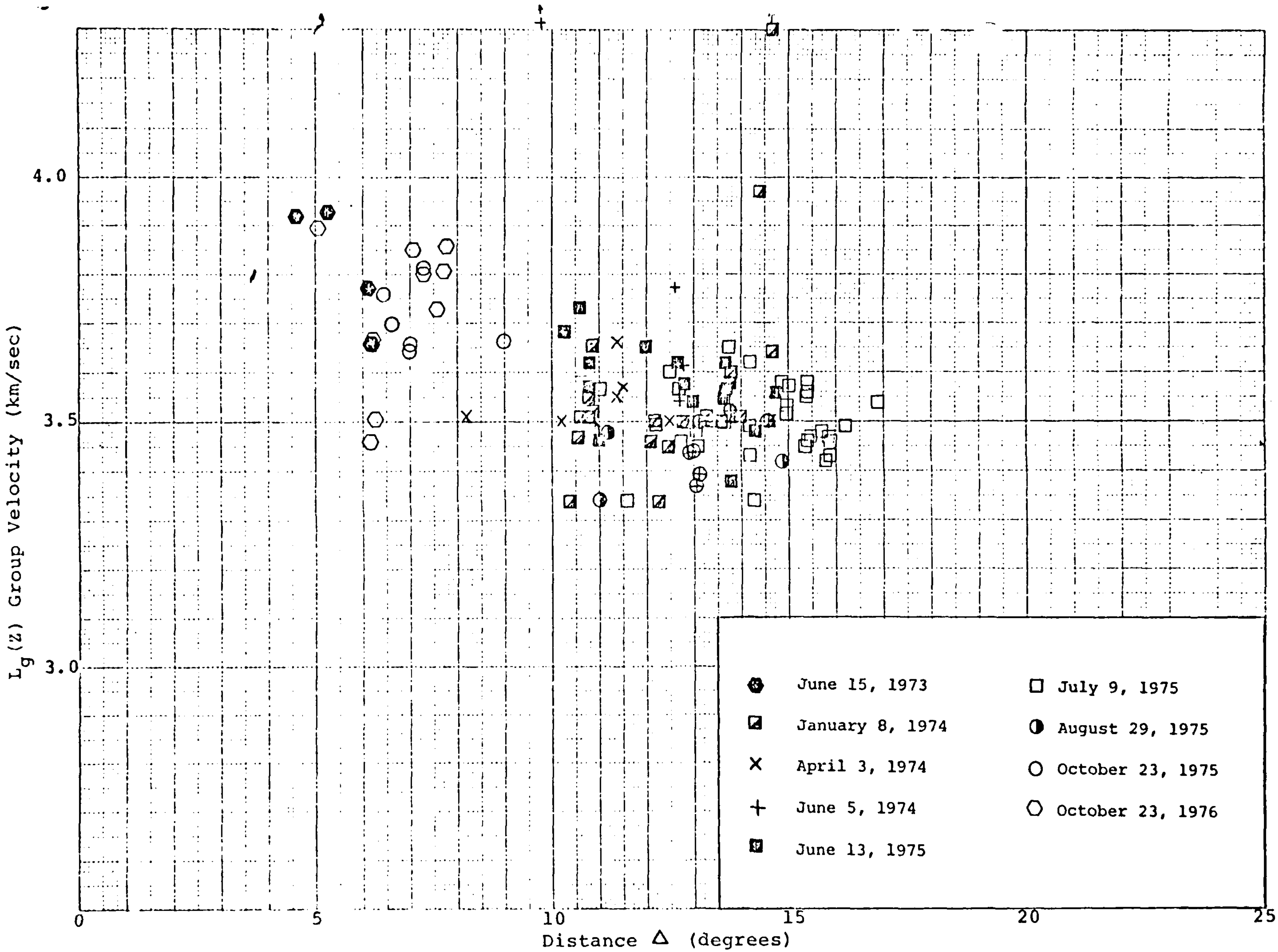

Figure 7. $L_g(Z)$ group velocity vs. distance as determined from NEUSSN station data.

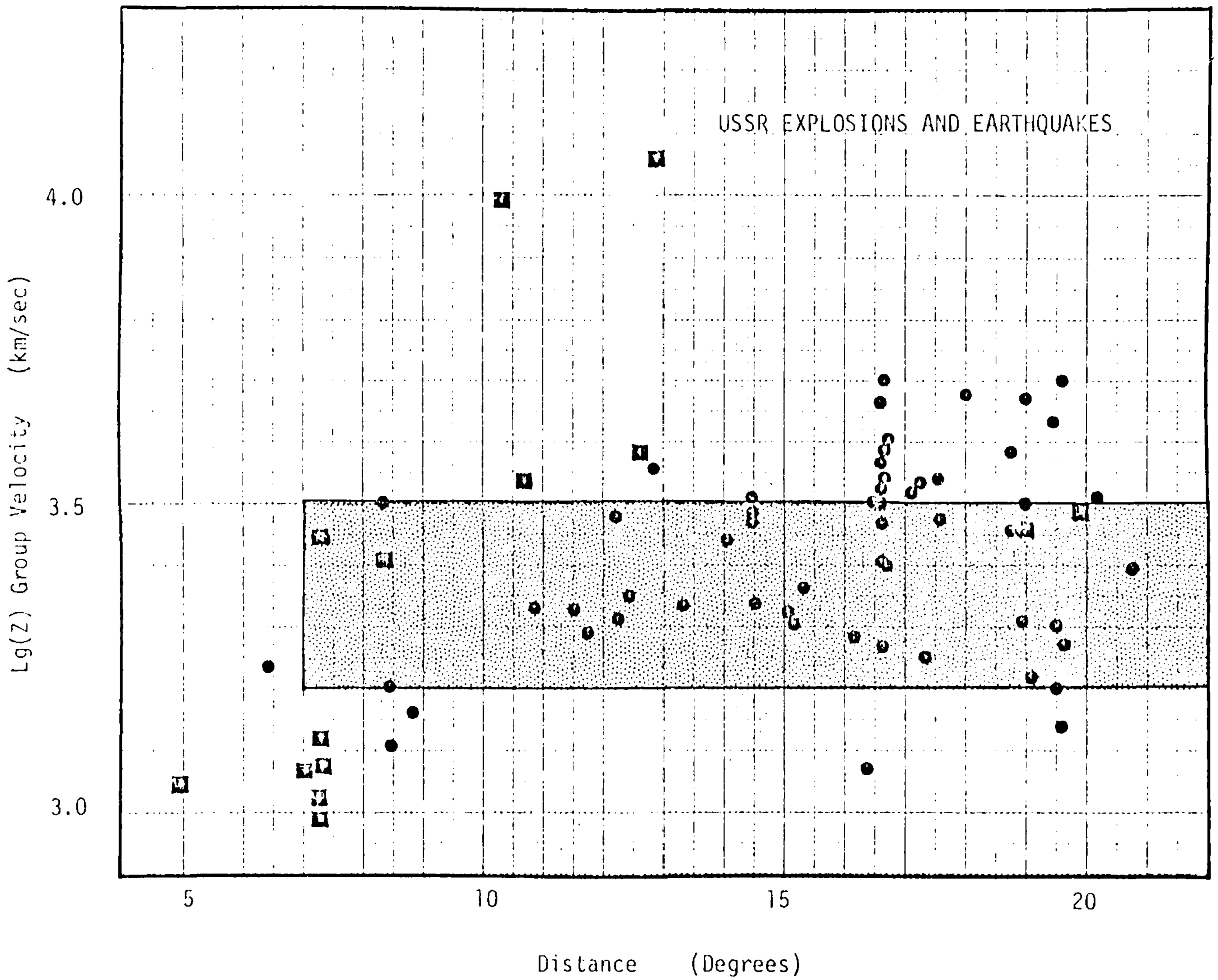

Figure 8. Composite of all Group Velocity Values for the Maximum Amplitude of Lg. The shaded area encloses the range of group velocities observed in the study of eastern USSR earthquakes.

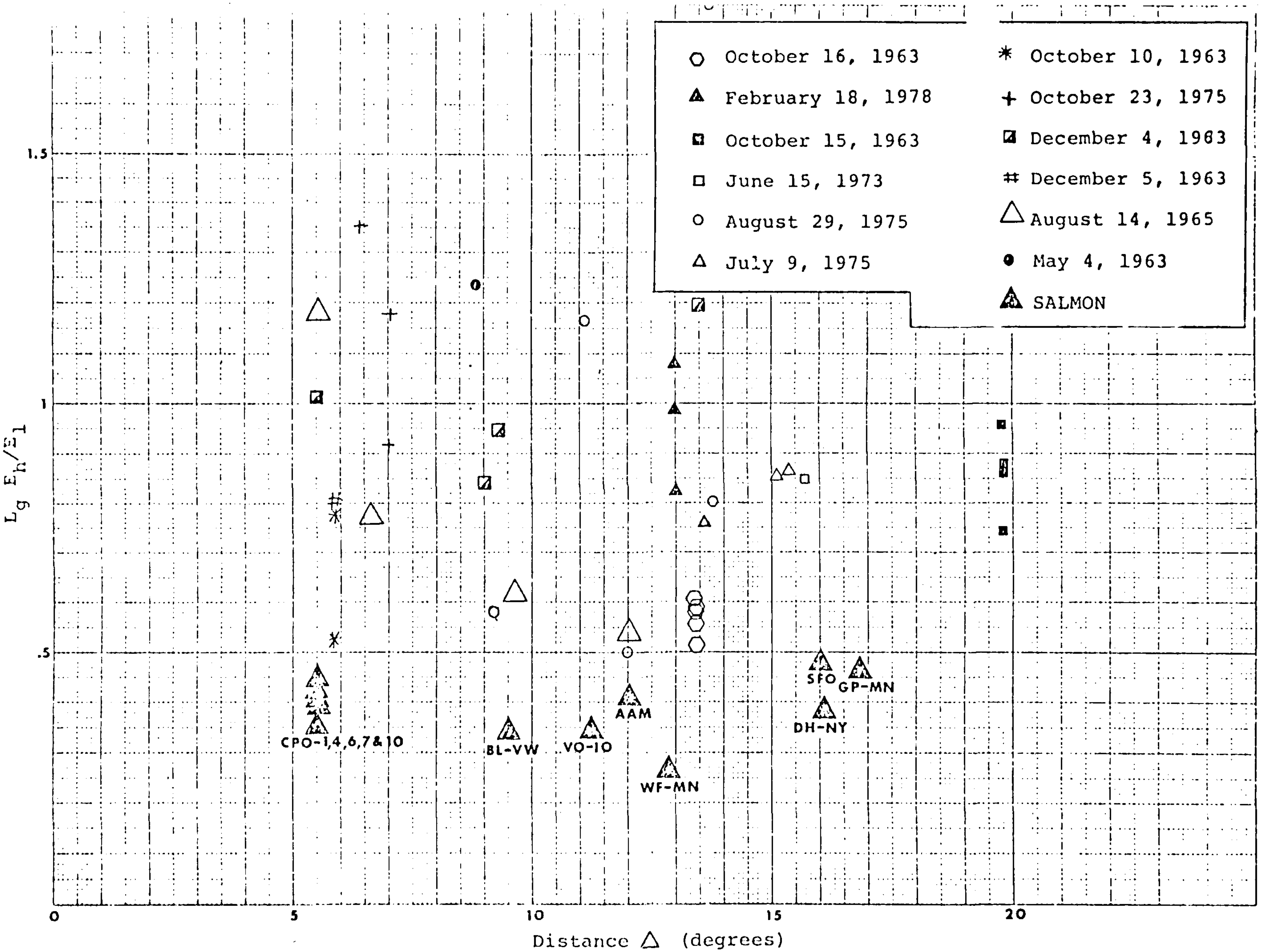

Figure 9. E_h/E_1 vs distance for 12 Eastern North American earthquakes and SALMON.

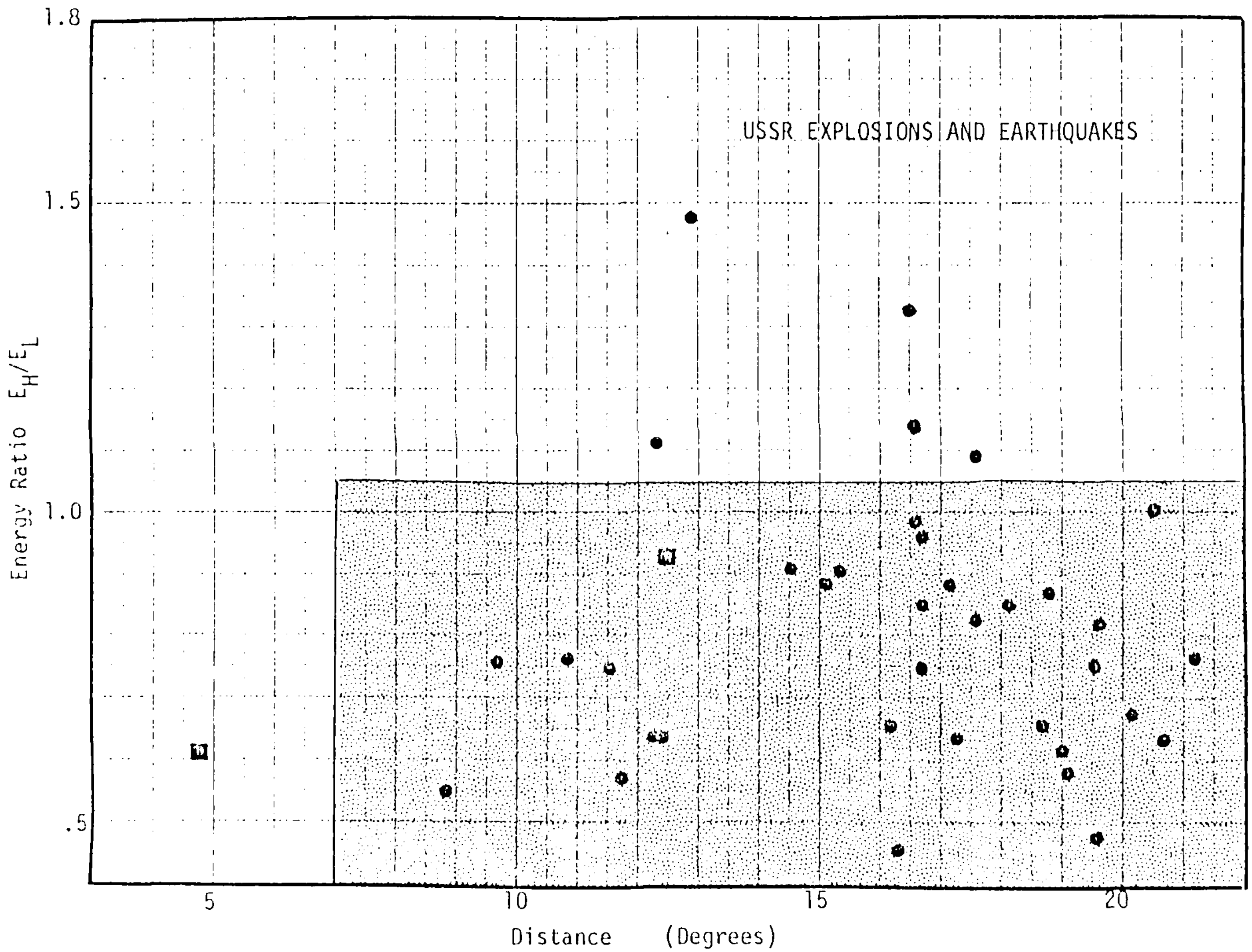

Figure 10. Energy Ratio Data for Explosions and Earthquakes in the USSR. Shaded area indicates range of values associated with earthquakes in the eastern USSR.

A/T-Z component-1 to 2 hertz L_g

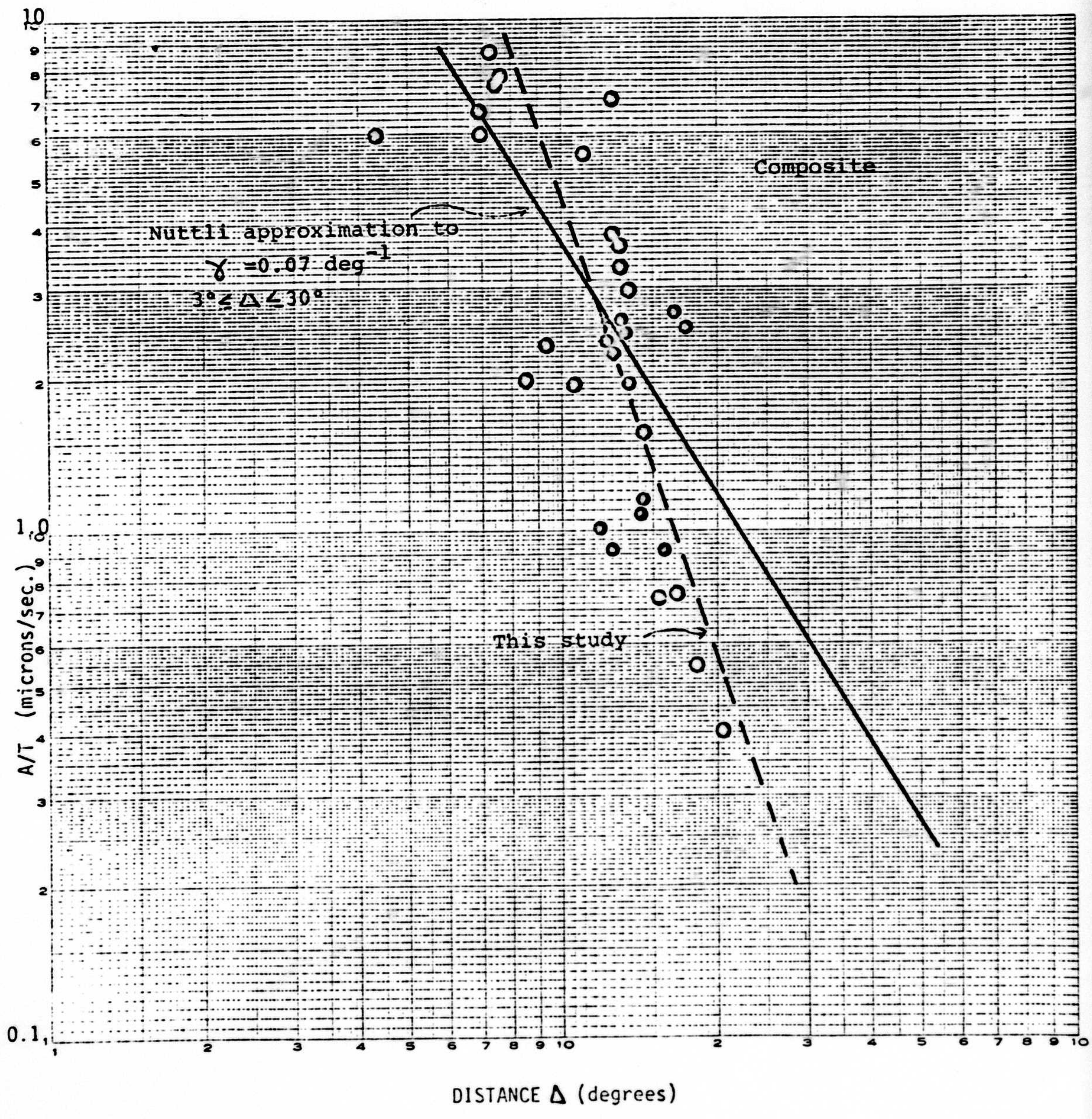

Figure 11.Composite L_g attenuation for the Eastern U.S.

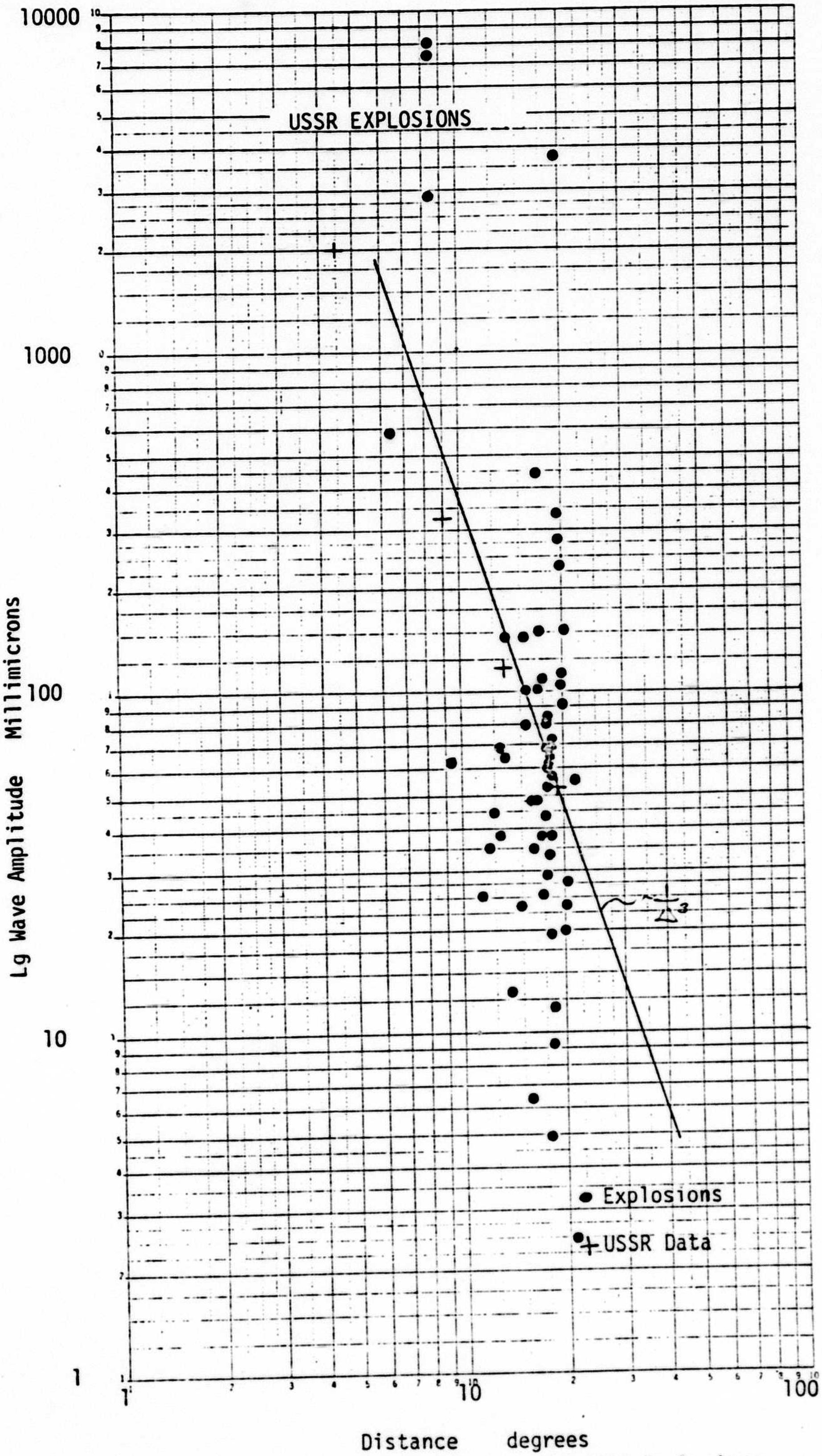

Figure 12. Lg Attenuation for USSR Explosions.

III. Magnitude-Yield Relation and Others

An accurate determination of the magnitude-yield relation is an important geophysical problem. Aside from its obvious application for estimating the yield of unknown nuclear tests by measuring the amplitudes of the observed seismic waves, a well-determined magnitude-yield relation may become one of the most useful tools for calibrating the seismic energy (especially at short periods) radiated by earthquakes. The task of casting this relation into a well defined form, however, is not an easy one. Difficulties can be traced to both the magnitude and the yield ends of the relation. Below we will describe some of the difficulties involved.

The amplitudes of the observed seismic waves can be significantly affected by several factors, such as (i) the medium and the burial depth of the source, (ii) the degree of seismic coupling between the source and the surrounding medium, and (iii) the local structures beneath the source and the receivers. The first and third factors have plagued seismologists for years, but these problems are currently being solved. To our knowledge, the second factor has not been studied extensively, its effects are therefore not well understood.

Several investigators have attempted to establish the magnitude-yield relation based on magnitudes that are determined from local/regional networks and/or a relatively small number of events. In view of the lack of completeness of these studies and the importance of this problem, we have decided to (i) undertake a comprehensive compilation of available published results that are relevant to the problem of yield-estimation, (ii) present the results from our compilation in a useful form, and (iii) improve the determination of body-wave magnitudes, in a statistical sense, by increasing the number of amplitude measurements at various epicentral distances. [ISC determines its body-wave magnitudes only if 3 or more stations report their amplitudes. It then applies the unified magnitude of Gutenberg (1956) to the amplitudes to determine the m_b. Few stations, however, have the habit of reporting their amplitudes to the ISC.]

Data.

Because of the large number (≥ 400) of nuclear tests in the United States and the Soviet Union, we have limited most of our data base to those underground nuclear explosions for which reports on their estimated yield exist. The U.S.

data used is derived from Springer and Kinnaman (1971, 1975), and the Soviet data, from Bolt (1976) and Dahlman and Israelson (1977). The magnitude determinations used are from Bolt (1976) and the International Seismological Centre (ISC) Bulletins. There are some doubts concerning the source reference of the estimated yield for the Soviet tests, compiled by Dahlman and Israelson, as well as the magnitude of the Soviet tests as reported by Bolt; we are in the process of uncovering these uncertainties.

Table IV represents a compilation of the U.S. explosion data used in this report. The table contains the name, data, origin time, location, and burial depth of the event; it also describes the rock-type surrounding the buried source (e.g. tuff, alluvium, rhyolite, etc.), the dimensions (volume, diameter, and height) of the collapse cavity, the body-wave magnitude (ISC), and the announced or estimated yield. Except for the magnitude, all the information was provided to Springer and Kinnaman (1971, 1975) by the U.S. Atomic Energy Commission (AEC). A compilation of the available Soviet data is outlined in Table V. This table consists of the date, computed origin time and location (Bolt, 1976), the body-wave magnitudes (from ISC and Bolt's compilation), and the estimated yield for these events (Dahlman and Israelson, 1977).

Based on the compilations in Table IV and V, we have made the following plots:

From the Soviet data: m_b (ISC and Bolt's) vs. estimated yield (Fig 13 and 14, respectively)

From the U.S. data:

a. m_b (ISC) vs. estimated yield (Fig. 15)
b. volume of collapse vs. estimated yield (Fig. 16
c. diameter and height of collapse center vs. estimated yield (Figures 17 and 18 respectively)
d. volume of collapse vs. depth of burial (Fig. 19)

Information on the locality and the rock-type of the test-site are also included whenever available.

Results and Discussion.

A comparison between the empirically determined and computed magnitude-yield relations in different media (cf. Fig. 7-8 of Bolt, 1976) and the data points in Fig. 13 and 15 shows that the U.S. data can be approximated closely by the curve for granite, whereas the Soviet data lies roughly between the curves for granite and water. Body-wave magnitudes taken from Bolt, on the other hand, show larger scatter than m_b(ISC) when plotted as a function of estimated yield (Figs.13 and 14). There is some indication that (i) events in the E. Kazakhstan are more efficient in generating seismic waves than the other test sites of the Soviet Union, and (ii) events situated in tuff and rhyolite generate waves more efficiently than those located in alluvium at the Nevada Test Site (NTS).

In plotting the collapse volume vs. the estimated yield (fig. 16), we divided the data into 3 groups: the first two groups (open and closed symbols) refer to events presented in Figure 15, while the third group (semi-filled symbols) consists of events that contain information on the collapse volume and the estimated yield but not on the body-wave magnitude. The first two groups are divided, somewhat arbitrarily, into normal (closed symbols) and anomalous (open symbols) events. The normal events lie closely together as a group, while the anomalous events appear to have unusually small collapse volumes for their estimated yields. Fig. 17 and 18 (the diameter and depth, respectively, of the collapse crater vs. estimated yield) were plotted from the same data set. It is quite interesting that except for the anomalous events, the diameter of the collapse crater can be approximated as being linearly proportional to the logarithm of the yield; the height of the crater, however, appears to be independent of the yield. Figure 19, which relates the collapse volume to the burial depth, is composed of the events found in Figure 17(or 18 as well as events without reports on their magnitude and yield. This figure seems to indicate three depth-dependent distributions: (i) the volume of collapse is independent of burial depth when the latter is less than about 900 ft., (ii) at depths between 900 and 2500 ft., the logarithm of the collapse volume is approximately linearly proportional to the burial depth, and (iii) for the three events at deeper than 4000 ft., the volume of collapse is again unpre-

dictable. A cautionary remark is deemed necessary at this point: the burial depth of the test charge is usually commensurate with its size; consequently, the collapse volume is probably a complex function of the local rock type, burial depth, and the actual yield.

In the remainng quarter of this fiscal year, we plan to conduct three projects: (i) to perform regression analysis for the data parameters mentioned above, (ii) to run a few simple statistical tests to evaluate the relative importance of the various parameters on the amplitudes of seismic waves and the dimensions of the collapse crater, and (iii) to upgrade the magnitude determination by incorporating additional amplitude readings from stations that did not furnish this information to the ISC.

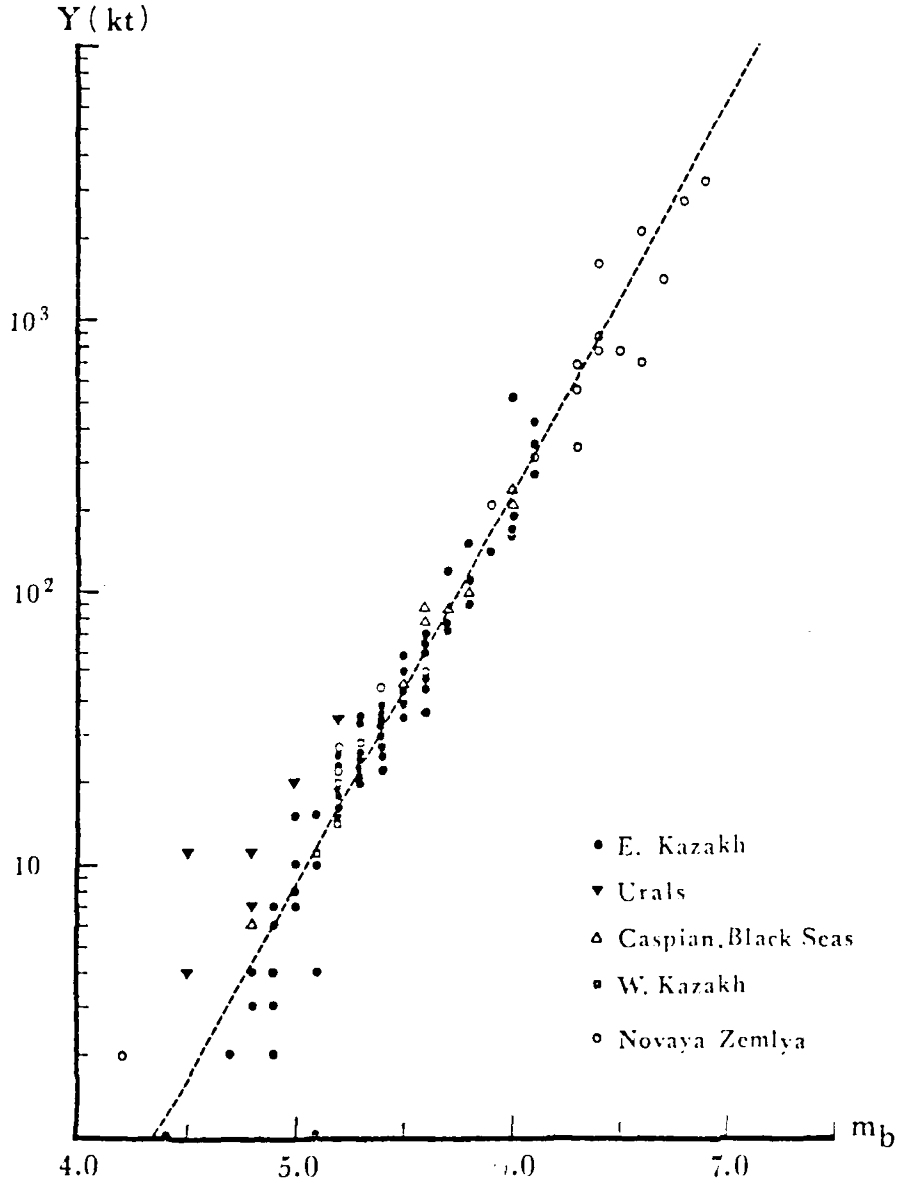

Figure 13. Body-wave magnitude (ISC) vs. yield for events in the USSR. The dashed line, $M_b = 0.75 \log_{10} Y + 4.345$, represents our preliminary, best-fitting relation between these two quantities.

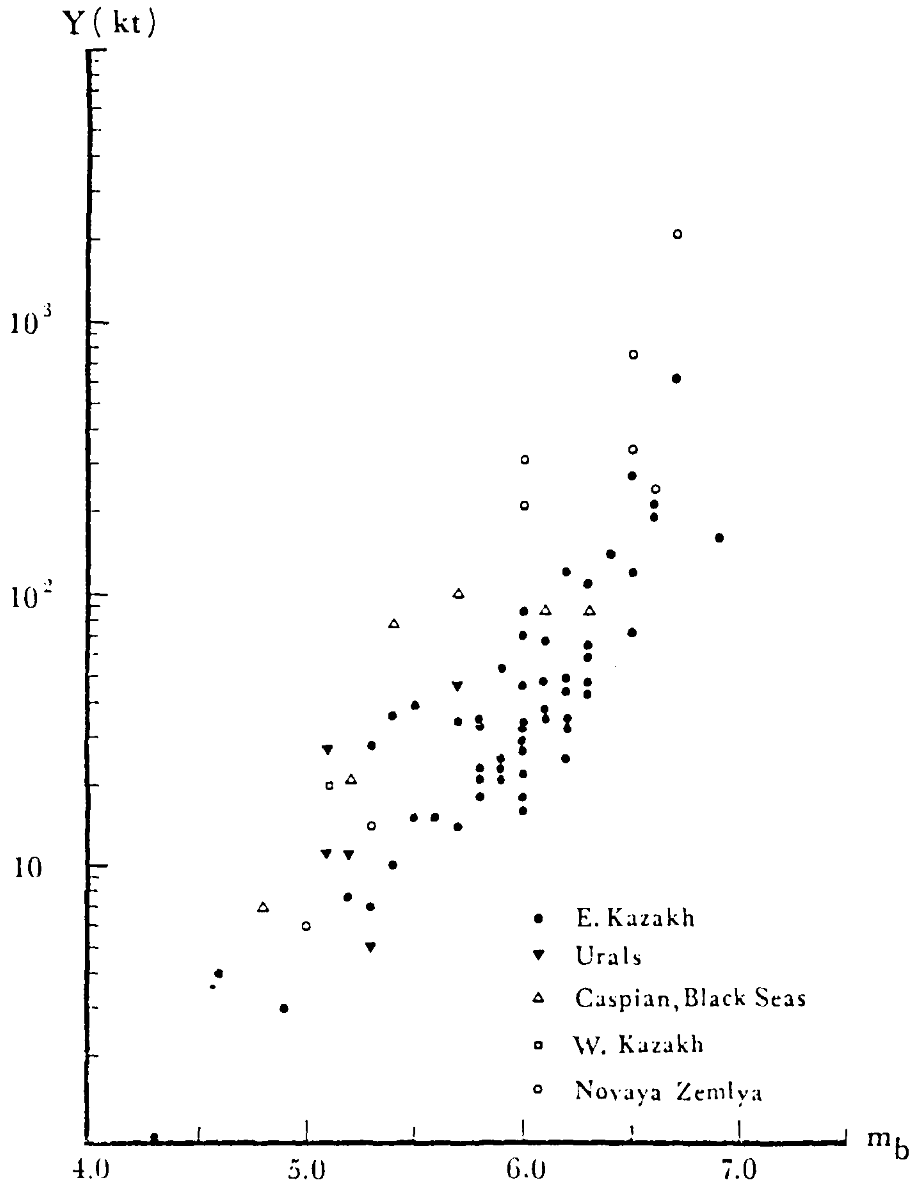

Figure 14. Body-wave magnitude (from Bolt's compilation) vs. yield for events in the USSR.

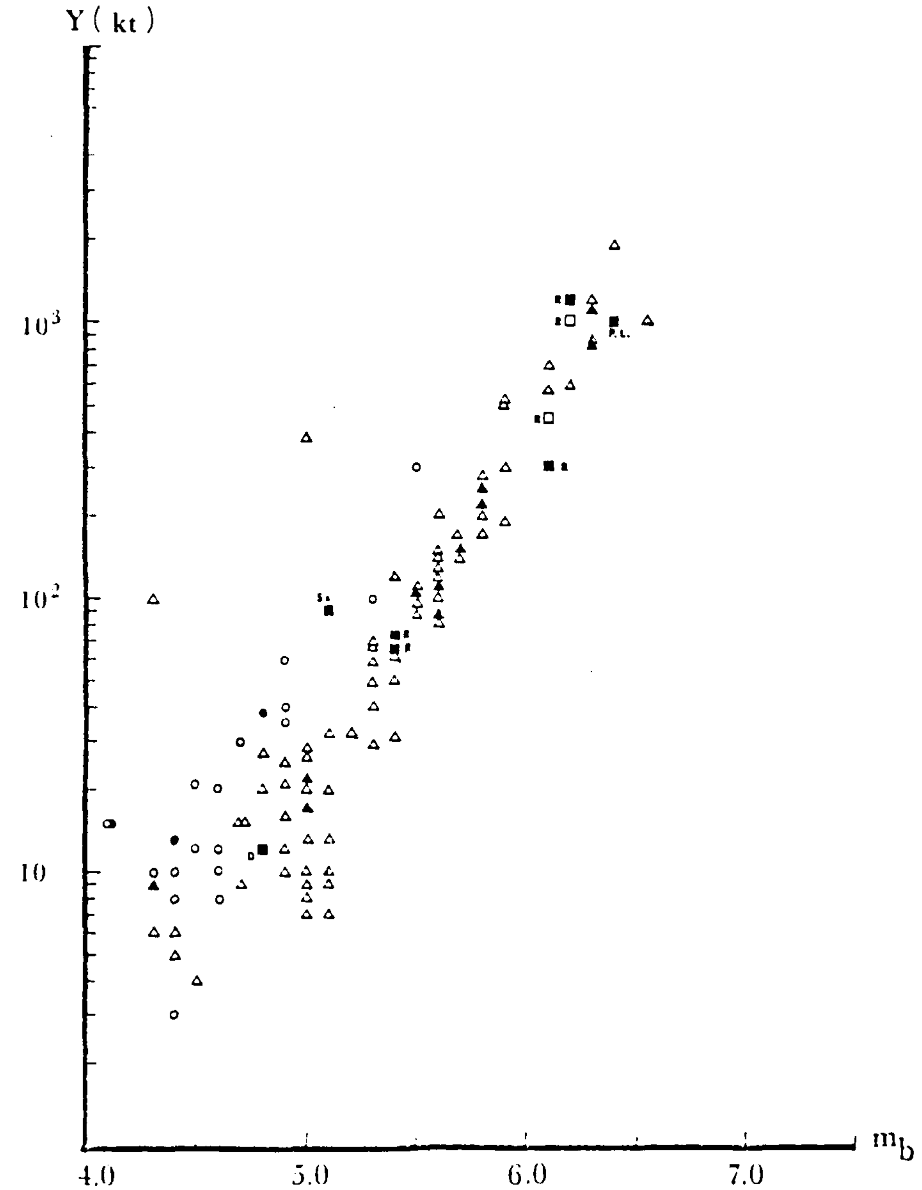

Figure 15. Body-wave magnitude (ISC) vs. yield for events in the US. Circles denote tests in alluvium; triangles, tests in tuff; and rectangles, tests in rhyolite (R), sandstone (Ss), or pillow lava (P.L.). The announced and estimated yields are indicated by filled and open symbols, respectively.

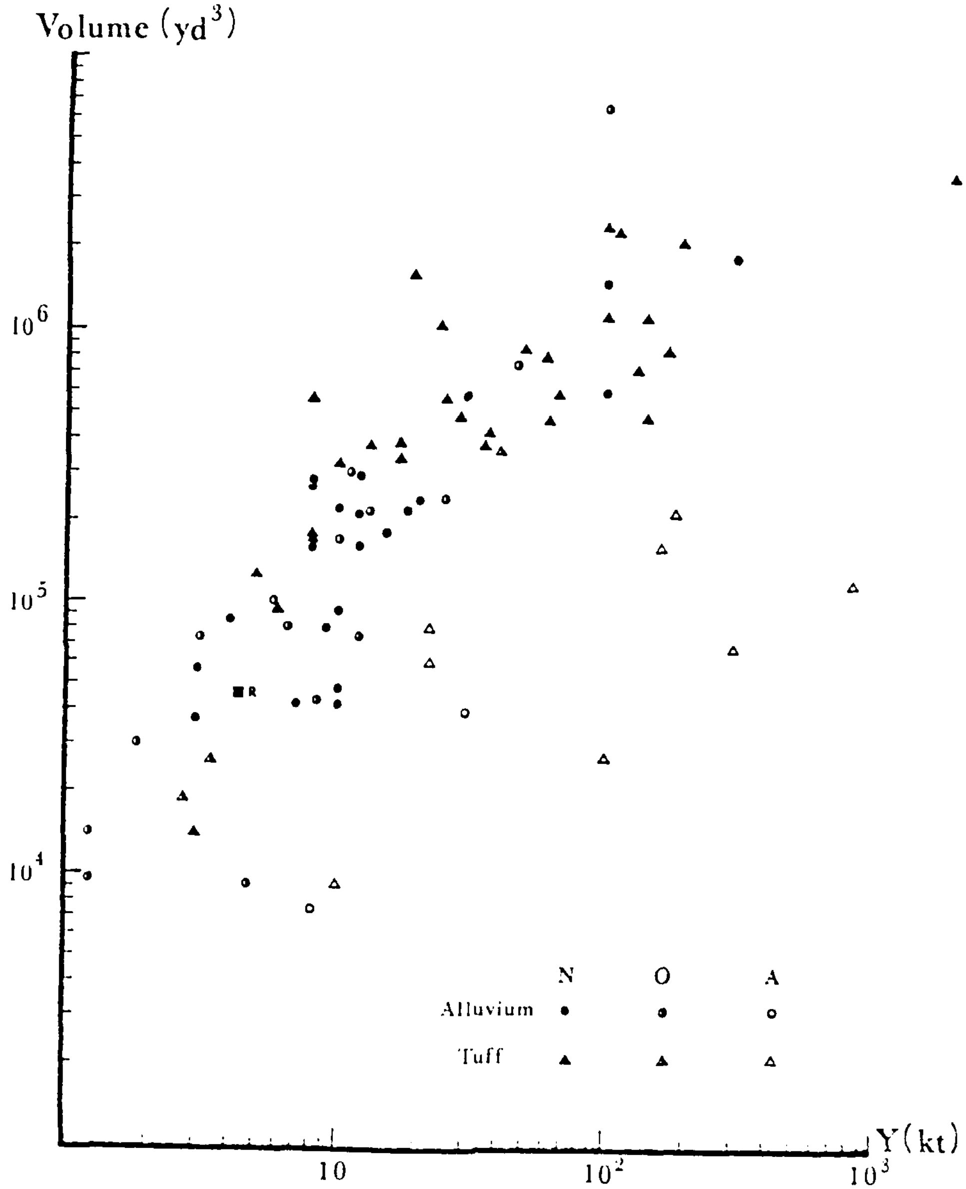

Figure 16. Volume of collapsed crater vs. estimated yield for events in the US. Open and filled symbols refer to events presented in Figure 3, whereas semi-filled symbols refer to events that contain information on the collapse volume and the estimated yield but not on the body-wave magnitude and therefore not plotted in Figure 3. Filled symbols denote normal (N) events which lie closely together as a group; open symbols, anomalous (A) events which appear to have unusually small collapse volumes for their estimated yields.

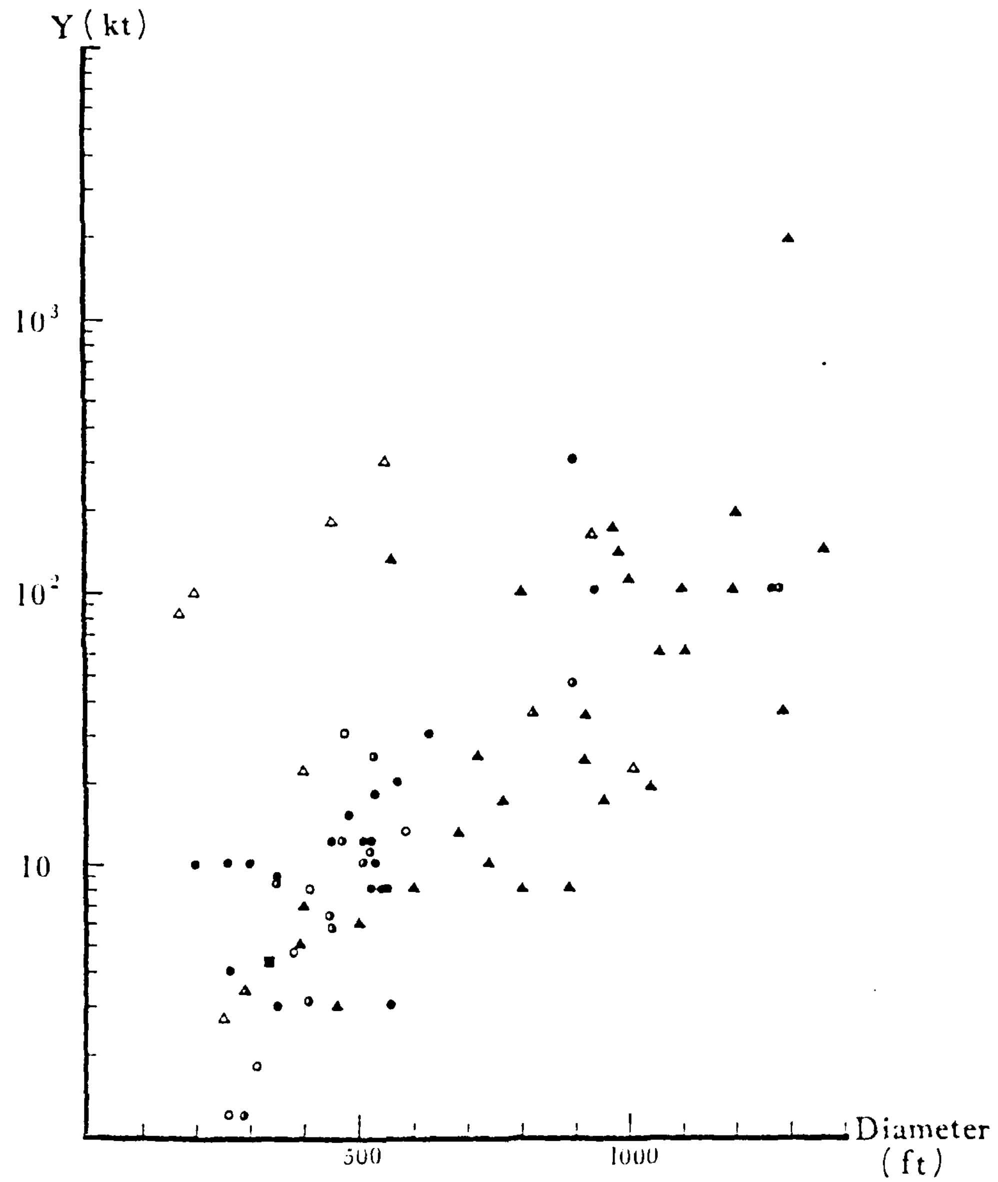

Figure 17. Diameter of the collapsed crater vs. estimated yield for events in the US. Except for the semi-filled symbols, the legends are similar to those in Figure 4.

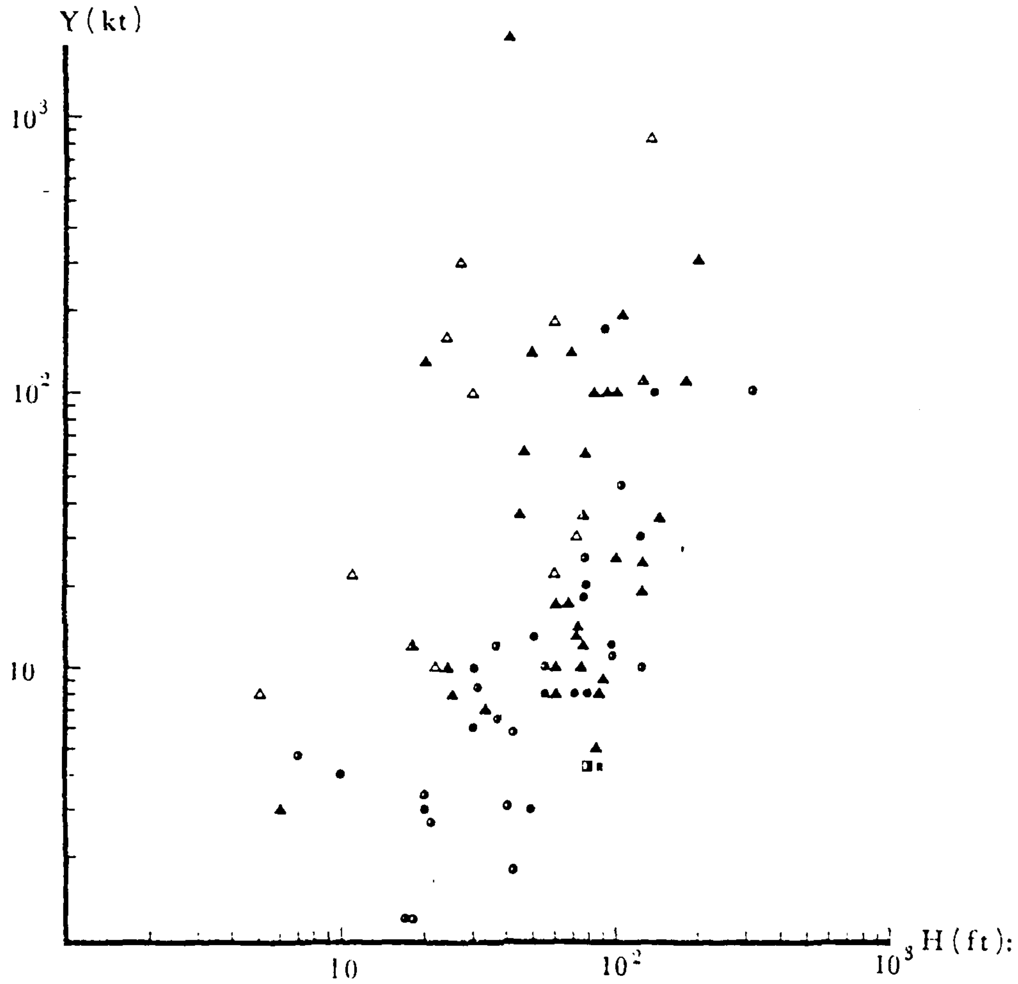

Figure 18. Height of the collapsed crater vs. estimated yield for events in the US. Except for the semi-filled symbols, the letends are similar to those in Figure 4.

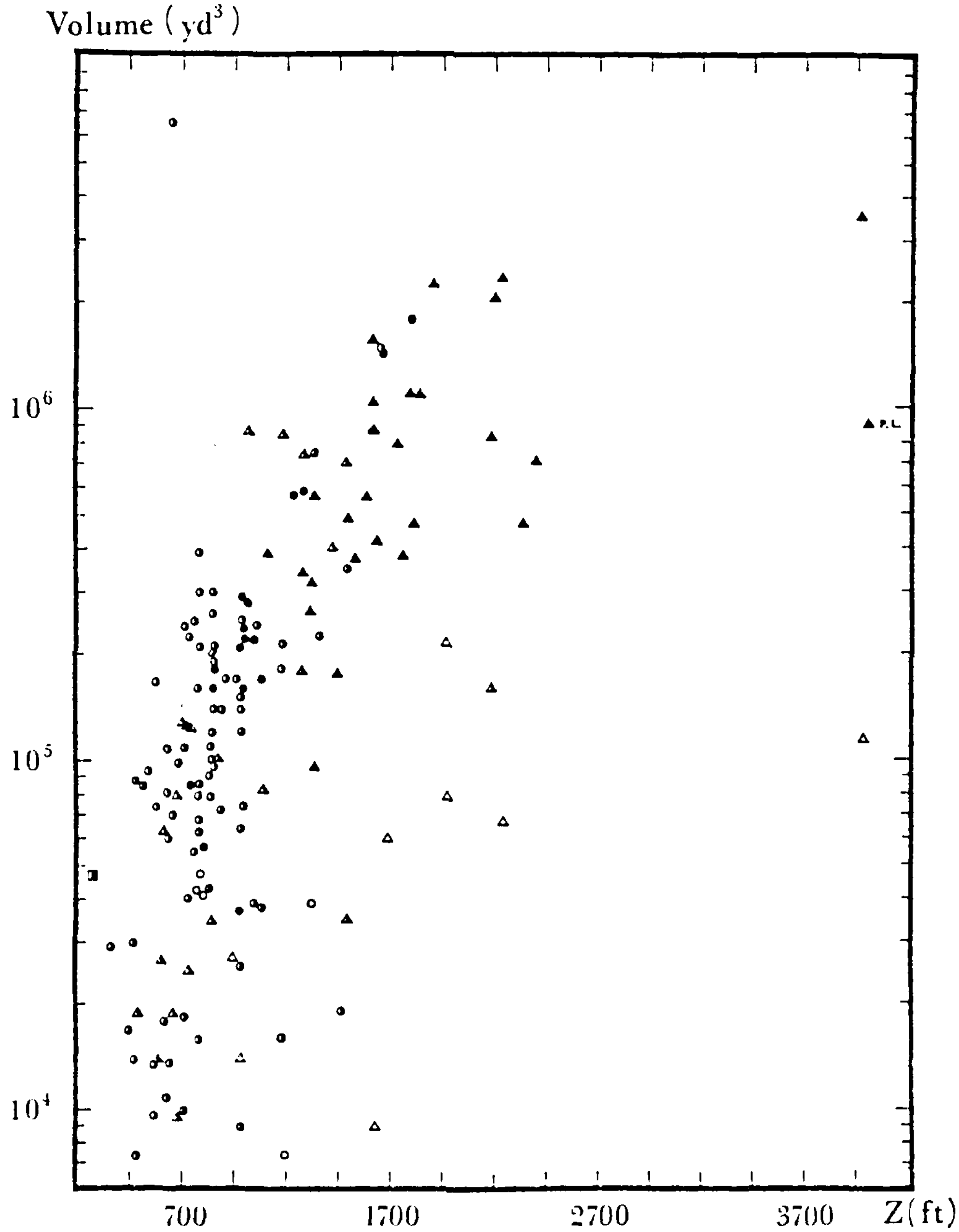

Figure 19. Volume of the collapsed crater vs. burial depth of the device for events in the US. Except for the semi-filled symbols, the legends are similar to those in Figure 4.

Table IV

U.S. Underground Nuclear Explosions

Year	Date	Shot Time	Device Depth (ft)	Epicenter Latitude (^{o}N)	Epicenter Longtitude (^{o}W)	Medium	Collapse Crater Volume (yd^3)	Collapse Crater Diam X Ht. (ft)	Announced	Estimated	M_b (ISC)	Type	Name
1967	0626	160000	1230	37.20	116.21	T				9	5.1		Midi Mist
cont.	0629	112500	1018	37.03	116.62	A	2.8 E05	542 X 79		8	4.6	N	Umber
	0727	130000	1587	37.15	116.05	T	5.6 E05	890 X 60		8	5.0	N	Stanley
	0818	201230	1089	37.01	116.04	A	1.7 E05	522 X 71		8	4.6	N	Bordeaux
	0831	163000	1463	37.18	116.21	T				9	5.0		Door Mist
	0907	134500	1700	37.15	116.05	T		1156 X 72		13	5.0		Yard
	0921	204500	572	37.17	116.04	A	1.33 E04	153 X 28	2.2			O	Marvel
	0927	170000	2188	37.10	116.05	T	8.3 E05	967 X 92		170	5.7	N	Zaza
	1018	143000	2343	37.12	116.06	T	4.74 E05	980 X 49		140	5.7	N	Lampher
	1025	143000	992	37.03	116.03	A	1.2 E05	525 X 48				O	Sazerac
	1108	150000	2200	37.09	116.04	T				7	5.1	N	Cobbler
1968	0119	181500	3200	38.63	116.21	T				1200	6.3		Faultless
	0221	153000	2116	37.12	116.05	T				200	5.8		Knox
	0229	170830	1345	37.18	116.21	T				20	5.0		Dorsal Fi
	0615	14000	2242	37.26	116.31	T	6.7 E04	548 X 27		300	5.9	A	Rickey
	0628	122200	1992	37.24	116.48	T				58	5.3		Chateau-gay
	0827	163000	794	36.88	115.93	A	1.6 E04	332 X 17				O	Diana Moon
	0906	140000	1909	37.14	116.05	T	2.24 E06	1000 X 182		110	5.5	N	Noggin
	0917	140000	1535	37.12	116.13	T	3.74 E05	682 X 72		13	5.1	N	Stoddard
	0924	170500	1092	37.20	116.21	T				10	5.0		Hudson Seal
	1003	142900	989	37.03	115.99	T	1.4 E04	460 X 6		3		A	Knife C
	1104	151500	1980	37.13	116.09	T	7.9 E04	400 X 60		22		A	Crew
	1115	154500	1191	37.03	116.03	A	7.2 E03	412 X 5		8		A	Knife B
	1120	180000	1010	37.01	116.21	T				12	4.9	N	Ming Vase
	1219	163000	4600	37.23	116.47	T			1100	1000	6.3		Benham
1969	0115	190000	810	37.15	116.07	A	5.64 E04	350 X 49		3			Packard
	0115	193000	1700	37.21	116.22	T				40	5.3		Wineskin
	0130	150000	1490	37.05	116.03	A		880 X 10		40	4.9		Vise
	0320	181200	998	37.02	116.03	A	2.2 E05	532 X 74		10	4.4	N	Barsac
	0321	143000	1525	37.13	116.09	A				35	4.9		Cotter
	0507	134500	1964	37.28	116.50	T	2.14 E05	450 X 60		180	5.5	A	Purse
	0527	141500	1689	37.07	115.99	T	6 E04	1004 X 11		22	5.0	A	Torrido
	0612	140000	994	37.01	116.03	A	2.9 E05	520 X 96		12	4.5	N	Tapper
	0716	130230	1346	37.12	116.05	T	9.57 E04	500 X 30		6		N	Ildrim
	0716	145500	1800	37.14	116.09	A	1.78 E06	898 X 201		300	5.5	N	Hutch
	0827	134500	784	37.02	116.04	A	6.8 E04	402 X 48				O	Pliers
	0916	143000	3800	37.31	116.46	T			1000	700	6.1		Jorum
	1002	220600	4000	51.42	-179.18	Pillow Lava	9.0 E05	2002 X 15	1000		6.4	O	Milrow
	1008	143000	2025	37.26	116.44	T		380 X 20		82	5.6		Pipkin
	1029	220151	2050	37.14	116.06	T		1000 X 75	110	140	5.6		Calabash
	1121	145200	1292	37.03	116.00	T				17	5.0	N	Picalilli
	1205	170000	1375	37.18	116.21	T				16	4.9		Diesel Train
	1217	150000	1807	37.08	116.00	T	4.7 E05	1102 X 46		61	5.4	N	Grape A
	1217	151500	1240	37.01	116.02	A	5.7 E05	632 X 123		30	4.7	N	Lovage
	1218	190000	1500	37.12	116.03	T	4.83 E05			28		N	Terrine
1970	0123	163000	998	37.14	116.04	T	2.36 E05	574 X 79		20		N	Ajo
	0204	170000	1819	37.10	116.03	T		1450 X 70		120	5.6		Grape B
	0205	150000	1450	37.16	116.04	T	1.74 E05	800 X 25	25	8		N	Labis
	0225	142838	1340	37.04	116.00	T	5.64 E05	720 X 100		25		N	Cumarin
	0226	153000	1287	37.12	116.06	A	5.91 E05	938 X 140		100	5.3	N	Yannigan
	0306	142401	950	37.02	116.09	T	2.7 E04	200 X 30	9.0	100	4.3	A	Cyathus
	0319	140330	988	37.00	116.02	A		455 X 35		6		O	Jal
	0323	230500	1839	37.09	116.02	T		1100 X 65		93	5.5		Shaper
	0326	190000	3957	37.30	116.53	T	3.54 E06	1300 X 40	1000	1900	6.4	N	Handley
	0421	143000	1125	37.05	115.99	T				6	4.4		Snubber
	0421	150000	1310	37.12	116.08	T	2.63 E05	600 X 85		8	4.6	N	Can
	0501	144000	870	37.13	116.03	T		515 X 43		6	4.3		Hod
	0505	153000	1330	37.22	116.18	T				28	5.0		Mint Leaf
	0515	133000	1455	37.16	116.04	T		790 X 157		39			Cornice
	0521	141500	1580	37.05	116.01	T				20	5.1		Morrones
	0526	150000	1743	37.11	116.06	T		975 X 160	105	110	5.5		Flask
	1014	143000	1639	37.07	116.00	T		1010 X 175		94	5.5		Tijeras
	1105	150000	1291	37.03	116.01	T		729 X 95		11			Abeytas
	1217	160500	2171	37.13	116.08	T		1100 X 100	220	170	5.8		Carpetbag
	1218	153000	994	37.17	116.10	T		500 X 80	10	32	5.1		Baneberry
1971	0623	153000	1493	37.02	116.02	T		616 X 21		10			Laguna
	0624	140000	1702	37.15	116.07	T		1000 X 78		40	4.9		Harebell
	0708	14000	1735	37.11	116.05	T		810 X 103	80	100			Miniata
	0818	140000		37.06	116.04	T		857 X 33		66	5.3		Algondones

Table IV

U.S. Underground Nuclear Explosions

Year	Date	Shot Time	Device Depth (ft)	Epicenter Latitude (^oN)	Epicenter Longtitude (^oW)	Medium	Collapse Crater Volume (yd^3)	Collapse Crater Diam X Ht. (ft)	Announced	Estimated	M_b (ISC)	Type	Name
1964	0625	133000	673	37.11	116.03	T	7.93 E04	416 X 47				O	Fade
cont.	0630	133300	847	37.17	116.06	A	7.88 E04	347 X 90		9		A	Dub
	0716	131500	1277	37.18	116.04	T	1.79 E05	536 X 65				O	Bye
	0904	181500	856	37.02	116.02	A	1.6 E05	450 X 74		12		N	Guanay
	1002	200300	1484	37.08	116.01	T				12	4.0	N	Auk
	1009	140000	1325	37.15	116.08	A	3.89 E04	475 X 72	38	30	4.0	A	Par
	1016	155930	849	37.04	116.02	A	1.2 E05	472 X 50				O	Barbel
	1105	150000	1319	37.17	116.07	Dolomite			12	9	4.8		Handcar
	1205	211500	1323	37.11	116.05	T	3.2 E05	740 X 60		10	4.8	N	Crepe
	1216	200000	592	37.03	116.01	A	1.4 E04	260 X 18	1.2			N	Parrot
	1216	201000	498	37.18	116.07	T	1.9 E04	254 X 21	2.7			N	Mudpack
1965	0114	160000	706	37.12	116.02	T	1.28 E05	450 X 60				O	Wool
	0204	153000	762	37.13	116.06	A	5.41 E04	360 X 45				O	Cashmere
	0216	173000	972	37.05	116.02	A	1.7 E05	510 X 55	10			N	Merlin
	0218	161847	588	36.82	115.95	A	1.66 E05	300 X 100				O	Wishbone
	0303	191300	2459	37.06	116.04	T				65			Wagtail
	0326	153408	1761	37.15	116.04	T	3.8 E05	920 X 185		35		N	Cup
	0405	210000	1466	37.03	116.02	A	1.9 E04	450 X 8				O	Kestrel
	0414	131400	280	37.28	116.52	R	4.69 E04	338 X 79	4.3			O	Palanquin
	0421	220000	1000	37.01	116.20	T				8	5.0		Gumdrop
	0507	154711	624	37.14	116.07	A	6.25 E04	385 X 30				O	Tee
	0521	130852	922	37.12	116.03	T	8.92 E05	630 X 148				O	Tweed
	0611	194500	593	37.04	116.02	A	9.5 E03	290 X 17	1.2			O	Petrel
	0723	170000	1741	37.10	116.03	T	7.9 E05	1055 X 77		60	5.4	N	Bronze
	0806	172330	1053	37.02	116.04	A	2.2 E05	526 X 77		18		N	Mauve
	0901	200800	990	37.02	116.01	A	2.1 E05	506 X 72		12	4.2	N	Screamer
	0910	171200	1494	37.08	116.02	T	3.5 E05	978 X 40				O	Charcoal
	1112	180000	791	37.05	116.02	A	8.6 E04	456 X 39				O	Sepia
	1203	151302	2236	37.16	116.05	T	2.33 E06	800 X 100				N	Corduroy
	1216	191500	1642	37.07	116.03	T	4.2 E05	1284 X 44		36	5.3	N	[illegible]
										32	5.2		Lampblack
1966	0118	183500	1842	37.09	116.02	T							
	0121	162800	1093	37.03	116.02	A	3.8 E04	464 X 16				O	Dovekie
	0203	181737	886	37.13	116.07	A	2.57 E04	260 X 27				O	Plaid II
	0224	155507	2204	37.27	116.43	T			16	7	5.0		Rex
	0307	184100	642	37.04	116.03	A	8.07 E04	408 X 58				O	Fintoot
	0318	[illegible]	1092	37.01	116.01	T	8.3 E04	458 X 39				O	Purple
	0406	135717	739	37.14	116.14	T	1.25 E05	386 X 85		5	4.4	N	Stutz
	0407	222730	742	37.02	115.99	T	2.5 E04	440 X 14				O	Tomato
	0414	141343		37.24	116.43	R			65	31	5.4	N	Duryea
	0425	183800	970	36.89	115.94	T				4	4.5		Pin Stripe
	0504	133217	646	37.14	116.14	A	1.09 E04	190 X 17				O	Traveler
	0505	140000	1001	37.05	116.04	A	1.6 E05	548 X 55	13	8	4.4	N	Cyclamen
	0512	193726	810	37.13	116.07	A	4.14 E04	300 X 24		10	4.3	A	Tapestry
	0513	133000	1800	37.09	116.03	T	1.1 E06	1196 X 83		100	5.6	N	Piranha
	0519	135628	2200	37.11	116.06	T	2.03 E06	1200 X 105		190	5.9	N	Dumont
	0527	200000	1106	37.18	116.10	T	3.9 E05	954 X 67	21	17	5.0	N	Discus Thrower
	0602	153000	1518	37.23	116.06	Granite			56		5.6		Pile Driver
	0603	140000	1839	37.07	116.03	T	1.1 E06	1362 X 69		140	5.7	N	Tan
	0615	180247	1494	37.17	116.05	D	7.01 E05	1300 X 60				O	Kankakee
	0625	171300	1057	37.15	116.07	A	2.41 E05	526 X 77	25			N	Vulcan
	0630	221500	2688	37.32	116.30	R		1300 X 35	300	450	6.1	N	Halfbeak
	0912	153001	835	36.88	115.95	A				12	4.6	O	Derringer
	0929	144530	750	37.17	116.05	A	8.54 E04	264 X 10		4		N	Newark
	1105	144500	650	37.17	116.05	A	1.36 E04	190 X 15				O	Simms
	1111	120000	782	37.13	116.05	A	6.33 E04	400 X 45				O	Ajax
	1118	150200	693	37.04	116.01	A	9.9 E04	452 X 50				O	Cerise
	1213	210000	800	36.88	115.94	A	4.74 E04	200 X 125		10	4.6	A	New Point
	1220	153000	825	37.30	116.41	T	(cylindrical)	170 X 135	825	830	6.3	A	Greeley
1967	0119	164500	1194	37.14	116.13	Dolomite	8.52 E05	500 X 180		49	5.3		Nash
	0120	174003	1636	37.16	116.00	Limestone		35 X 135		29	5.3		Bourban
	0208	151500	844	37.17	116.05	A	9.07 E04	260 X 30		10	4.6	A	Ward
	0223	188400	981	37.02	116.02	A	3.7 E04	560 X 20		3	4.4	A	Persimmon
	0223	185000	2400	37.13	116.07	T	7.12 E05	900 X 40		130	5.6	N	Agile
	0302	150000	890	37.17	116.05	A	7.24 E04	460 X 12				O	River III
	0407	150000	889	37.05	116.02	A	1.4 E05	510 X 52				O	Fawn
	0421	150900	789	37.02	116.06	A	4.2 E04	400 X 33		7		A	Chocolate
	0427	144500	719	37.14	116.06	A	1.84 E04	114 X 12				O	Effendi
	0510	134000	1639	37.08	115.99	T	9 E03	184 X 22		10	4.9	A	Mickey
	0520	150000	2449	37.13	116.06	T		1120 X 148	250	230	5.8		Commodore
	0523	140000	3207	37.27	116.37	T			150	140	5.7		Scotch
	0526	150002	2069	37.25	116.48	R			71	47	5.4		Knickerbocker

Table IV

U.S. Underground Nuclear Explosions

Year	Date	Shot Time	Device Depth (ft)	Epicenter Latitude (°N)	Epicenter Longtitude (°W)	Medium	Collapse Crater Volume (yd^3)	Collapse Crater Diam X Ht. (ft)	Announced	Estimated	M_b (ISC)	Type	Name
1967	0626	160000	1230	37.20	116.21	T				9	5.1		Midi Mist
cont.	0629	112500	1018	37.03	116.62	A	2.8 E05	542 X 79		8	4.6	N	Umber
	0727	130000	1587	37.15	116.05	T	5.6 E05	890 X 60		8	5.0	N	Stanley
	0818	201230	1089	37.01	116.04	A	1.7 E05	522 X 71		8	4.6	N	Bordeaux
	0831	163000	1463	37.18	116.21	T				9	5.0		Door Mist
	0907	134500	1700	37.15	116.05	T		1156 X 72		13	5.0		Yard
	0921	204500	572	37.17	116.04	A	1.33 E04	153 X 28	2.2			0	Marvel
	0927	170000	2188	37.10	116.05	T	8.3 E05	967 X 92		170	5.7	N	Zaza
	1018	143000	2343	37.12	116.06	T	4.74 E05	980 X 49		140	5.7	N	Lampher
	1025	143000	992	37.03	116.03	A	1.2 E05	525 X 48				0	Sazerac
	1108	150000	2200	37.09	116.04	T				7	5.1	N	Cobbler
1968	0119	181500	3200	38.63	116.21	T				1200	6.3		Faultless
	0221	153000	2116	37.12	116.05	T				200	5.8		Knox
	0229	170830	1345	37.18	116.21	T				20	5.0		Dorsal Fin
	0615	14000	2242	37.26	116.31	T	6.7 E04	548 X 27		300	5.9	A	Rickey
	0628	122200	1992	37.24	116.48	T				58	5.3		Chateau-gay
	0827	163000	794	36.88	115.93	A	1.6 E04	332 X 17				0	Diana Moon
	0906	140000	1909	37.14	116.05	T	2.24 E06	1000 X 182		110	5.5	N	Noggin
	0917	140000	1535	37.12	116.13	T	3.74 E05	682 X 72		13	5.1	N	Stoddard
	0924	170500	1092	37.20	116.21	T				10	5.0		Hudson Seal
	1003	142900	989	37.03	115.99	T	1.4 E04	460 X 6		3		A	Knife C
	1104	151500	1980	37.13	116.09	T	7.9 E04	400 X 60		22		A	Crew
	1115	154500	1191	37.03	116.03	A	7.2 E03	412 X 5		8		A	Knife B
	1120	180000	1010	37.01	116.21	T				12	4.9	N	Ming Vase
	1219	163000	4600	37.23	116.47	T			1100	1000	6.3		Benham
1969	0115	190000	810	37.15	116.07	A	5.64 E04	350 X 49		3			Packard
	0115	193000	1700	37.21	116.22	T				40	5.3		Wineskin
	0130	150000	1490	37.05	116.03	A		880 X 10		40	4.9		Vise
	0320	181200	998	37.02	116.03	A	2.2 E05	532 X 74		10	4.4	N	Barsac
	0321	143000	1525	37.13	116.09	A				35	4.9		Coffer
	0507	134500	1964	37.28	116.50	T	2.14 E05	450 X 60		180	5.5	A	Purse
	0527	141500	1689	37.07	115.99	T	6 E04	1004 X 11		22	5.0	A	Torrido
	0612	140000	994	37.01	116.03	A	2.9 E05	520 X 96		12	4.5	N	Tapper
	0716	130230	1346	37.12	116.05	T	9.57 E04	500 X 30		6		N	Ildrim
	0716	145500	1800	37.14	116.09	A	1.78 E06	898 X 201		300	5.5	N	Hatch
	0827	134500	784	37.02	116.04	A	6.8 E04	402 X 48				0	Pliers
	0916	143000	3800	37.31	116.46	T			1000	700	6.1		Jorum
	1002	220600	4000	51.42	-179.18	Pillow Lava	9.0 E05	2002 X 15	1000		6.4	0	Milrow
	1008	143000	2025	37.26	116.44	T		380 X 20		82	5.6		Pipkin
	1029	220151	2050	37.14	116.06	T		1000 X 75	110	140	5.6		Calabash
	1121	145200	1292	37.03	116.00	T				17	5.0	N	Picalilli
	1205	170000	1375	37.18	116.21	T				16	4.9		Diesel Train
	1217	150000	1807	37.08	116.00	T	4.7 E05	1102 X 46		61	5.4	N	Grape A
	1217	151500	1240	37.01	116.02	A	5.7 E05	632 X 123		30	4.7	N	Lovage
	1218	190000	1500	37.12	116.03	T	4.83 E05			28		N	Terrine
1970	0123	163000	998	37.14	116.04	T	2.36 E05	574 X 79		20		N	Ajo
	0204	170000	1819	37.10	116.03	T		1450 X 70		120	5.6		Grape B
	0205	150000	1450	37.16	116.04	T	1.74 E05	800 X 25	25	8		N	Labis
	0225	142838	1340	37.04	116.00	T	5.64 E05	720 X 100		25		N	Cumarin
	0226	153000	1287	37.12	116.06	A	5.91 E05	938 X 140		100	5.3	N	Yannigan
	0306	142401	950	37.02	116.09	T	2.7 E04	200 X 30	9.0	100	4.3	A	Cyathus
	0319	140330	988	37.00	116.02	A		455 X 35		6		0	Jal
	0323	230500	1839	37.09	116.02	T		1100 X 65		93	5.5		Shaper
	0326	190000	3957	37.30	116.53	T	3.54 E06	1300 X 40	1000	1900	6.4	N	Handley
	0421	143000	1125	37.05	115.99	T				6	4.4		Snubber
	0421	150000	1310	37.12	116.08	T	2.63 E05	600 X 85		8	4.6	N	Can
	0501	144000	870	37.13	116.03	T		515 X 43		6	4.3		Hod
	0505	153000	1330	37.22	116.18	T				28	5.0		Mint Leaf
	0515	133000	1455	37.16	116.04	T		790 X 157		39			Cornice
	0521	141500	1580	37.05	116.01	T				20	5.1		Morrones
	0526	150000	1743	37.11	116.06	T		975 X 160	105	110	5.5		Flask
	1014	143000	1839	37.07	116.00	T		1010 X 175		94	5.5		Tijeras
	1105	150000	1291	37.03	116.01	T		729 X 95		11			Abeytas
	1217	160500	2171	37.13	116.08	T		1100 X 100	220	170	5.8		Carpetbag
	1218	153000	994	37.17	116.10	T		500 X 80	10	32	5.1		Baneberry
1971	0623	153000	1493	37.02	116.02	T		616 X 21		10			Laguna
	0624	140000	1702	37.15	116.07	T		1000 X 78		40	4.9		Harebell
	0708	14000	1735	37.11	116.05	T		810 X 103	80	100			Mintata
	0818	140000		37.06	116.04	T		857 X 33		[illegible]	[illegible]		[illegible]

Table IV

U.S. Underground Nuclear Explosions

Year	Date	Shot Time	Device Depth (ft)	Epicenter Latitude (^oN)	Epicenter Longtitude (^oW)	Medium	Collapse Crater Volume (yd^3)	Collapse Crater Diam X Ht. (ft)	Announced	Estimated	M_b (ISC)	Type	Name
1971 cont.	1008	143000	1240	37.11	116.04	T		840 X 26		7			Cathay
	1106	220000	5875	51.47	-179.11	Basalt		3600 X 55	5000		6.6		Cannikin
	1214	210959	1085	37.12	116.09	A		372 X 41		24			Chaenactis
1972	0517	14100	1059	37.12	116.09	A		336 X 48		8			Zinnia
	0720	171600	1391	37.21	116.18	T				21	4.9		Diamond Sculls
	0921	153000	1838	37.08	116.04	T		1350 X 90		130	5.6		Oscuro
	0926	143000	970	37.12	116.09	A		388 X 51	15	15	4.1		Delphinium
	1221	201500	2258	37.14	116.08	T		584 X 97		27	4.8		Flax
1973	0308	161000	1866	37.10	116.03	T		1116 X 41		67	5.3		Miera
	0425	222500	1486	37.00	116.03	A				21	4.5		Angus
	0426	171500	1850	37.12	116.06	T		1150 X 125	85	120	5.6		Starwort
	0517	160000		39.79	108.37	Sandstone			90		5.1		Rio Blanco
	0605	170000	1284	37.18	116.21	T				26	5.0		Dido Queen
	0606	130000	3490	37.24	116.35	T				570	6.1		Almendro
	0628	191512	1530	37.15	116.09	A				60	4.9		Portulaca
	1012	170000	1350	37.20	116.20	T				9	4.7		Husky Ace
1974	0227	170000		37.10	116.05					150	5.6		Latir
	0619	160000		37.20	116.19					20	4.8		Ming Blade
	0710	160000		37.07	116.03					170	5.7		Escabosg
	0830	150000		37.15	116.08					200	5.6		Portman-teau
	0926	150500		37.13	116.07					100	5.5		Stanyan
1975	0228	151500		37.11	116.06					135	5.6		Topgallant
	0307	150000		37.13	116.08					120	5.4		Cabrillo
	0405	194500		37.19	116.21					20	4.9		Dining Car
	0424	141000		37.12	116.09					9	4.5		Edan
	0514	140000	2510	37.22	116.47					380	5.0		Tybo
	0603	142000	2398	37.34	116.52					275	5.8		Stilton
	0603	144000	2090	37.09	116.04					160	5.6		Mizzen
	0619	130000	2992	37.35	116.32					520	5.9		Mast
	0626	123000	4301	37.28	116.37					750	6.1		Camembert
	1024	171126	440	37.22	116.18					15	4.7		Husky Pup
	1028	143000	4150	37.29	116.41					1200	6.2		Kasseri
	1120	150000	2680	37.22	116.37					500	5.9		Inlet
	1220	200000	2349	37.13	116.06					160	5.6		Chiberta
1976	0103	191500	4761	37.30	116.33					600	6.2		Muenster
	0204	142000	2100	37.07	116.03					200	5.6		Keelson
	0204	144000	2149	37.11	116.04					150	5.6		Esrom
	0212	144500	3999	37.21	116.49					900	6.1		Fontina
	0214	113000	3229	37.24	116.42					350	5.8		Cheshire
	0309	140000	2851	37.31	116.36					350	5.8		Estuary
	0314	123000	4177	37.31	116.47					900	6.2		Colby
	0317	141500	2884	37.26	116.31					500	6.0		Pool
	0317	144500	2559	37.11	116.05					200	5.8		Strait

Table V

Year	Date	Origin Time	Latitude (^{o}N)	Longitude (^{o}E)	m_b (Bolt's)	Announced	Estimated	m_b (ISC)	Location
1964	0315	75958	49.70	78.00	6.2		49	5.6	
	0516	60058	49.90	78.30	6.2		44	5.6	
	0719	55959	49.90	78.10	6.0		29	5.4	
	0918	75955	72.90	55.20			2	4.2	N.Z.
	1025	75959	73.50	53.70	5.3		14	5.1	N.Z.
	1116	55957	49.70	78.00	6.1		49	5.6	
1965	0115	55959	49.89	78.97	7.0	125	110	5.8	
	0303	61457	49.82	78.07	6.0		34	5.5	
	0511	63958	49.79	77.92			6	4.9	
	0617	24458	49.97	78.07	5.8		21	5.2	
	0917	35958	49.81	78.05	5.5		15	5.2	
	1008	55959	49.89	78.05	5.8		34	5.4	
	1121	45758	49.77	78.06	6.1		47	5.6	
	1224	45958	49.88	78.04			7	5.0	
1966	0213	45758	49.82	78.13	6.5		270	6.1	
	0320	54958	49.70	78.00			170	6.0	
	0421	35758	49.81	78.05	5.3		28	5.3	
	0507	35758	49.74	77.90			4	4.8	
	0629	65758	49.93	78.01			36	5.6	
	0721	35758	49.70	78.00	5.9		24	5.3	
	0805	35758	49.90	78.00	6.1		29	5.4	
	0819	35301	50.40	77.90	4.6		4	5.1	
	0907	35158	49.90	78.00			4	4.8	
	0930·	55953	38.80	64.50	5.3	30			Uzbekistan
	1019	35758	49.75	78.03	6.3		65	5.6	
	1027	55758	73.44	54.75	6.5		770	6.4	N.Z.
	1218	45758	49.93	77.73	6.5		120	5.8	
1967	0226	35758	49.78	78.12	6.6		210	6.0	
	0325	55759	49.77	78.08	5.9		21	5.3	
	0420	40758	49.74	78.12	6.3		58	5.5	
	0528	40758	49.81	78.11	6.2		32	5.4	
	0629	25658	49.87	78.10			27	5.3	
	0715	32657	49.83	78.11	6.0		27	5.4	
	0804	65758	49.82	78.05	5.8		23	5.3	
	0916	40358	50.01	77.82	6.0		22	5.3	
	0922	50358	50.03	77.61	6.0		16	5.2	
	1017	50358	49.82	78.10	6.1		67	5.6	
	1021	45958	73.37	54.81	6.0		210	5.9	N.Z.
	1030	60358	49.84	78.11	6.0		33	5.3	
	1122	40357	49.90	77.30			3	4.8	
	1208	60357	49.84	78.22			22	5.4	
1968	0107	34658	49.81	78.02			10	5.1	
	0424	103557	49.83	78.08			7	5.0	
	0611	30558	49.84	78.16	5.8		18	5.2	
	0619	50557	49.96	79.09	6.5		35	5.4	
	0701	40202	47.92	47.95	5.7		46	5.5	N. Caspian Sea
	0712	120757	49.67	78.12	5.9		23	5.3	
	0820	40558	50.00	78.00			4	4.8	
	0905	40557	49.76	78.14	6.2		35	5.4	
	0929	34258	49.77	78.19	6.3		110	5.8	
	1107	100205	73.40	54.86	6.0		310	6.1	N Z.
	1109	25358	49.79	78.04			4	4.9	
	1218	50157	49.72	78.06	5.7		14		
1969	0307	82658	49.81	78.15	6.3		47	5.6	
	0516	40257	49.77	78.15	6.0		18	5.2	
	0531	50157	49.98	77.73	6.2		25	5.3	
	0704	24657	49.75	78.19	6.0		22	5.2	
	0723	24658	49.87	78.32	6.1		38	5.4	
	0902	45957	57.41	54.86	5.2	8	11	4.8	Urals
	0908	45956	57.36	55.11	5.2	8	11	4.8	Urals
	0926	65956	45.89	42.47	5.4		78	5.6	N. Caspian Sea
	1001	40258	49.81	78.21	5.9		21	5.2	
	1014	70006	73.40	54.81	6.5		340	6.3	N.Z.
	1130	33257	49.92	79.00	6.9		160	6.0	
	1206	70257	43.83	54.78	5.7		100	5.8	E. Caspian Sea
	1228	34658	50.00	77.82	6.5		72	5.7	
	1229	40158	49.73	78.15			1	5.1	
1970	0129	70258	49.80	78.21	5.9		52	5.5	
	0327	50257	49.76	78.01	5.4		10	5.0	
	0625	45952	52.20	55.69	5.3		5		Urals
	0628	15758	49.83	78.25	6.2		120	5.7	
	0721	30257	49.95	77.75	6.0		29	5.4	
	0724	35657	49.80	78.17	5.8		21	5.3	
	0906	40257	49.77	78.09	6.0		46	5.4	
	1014	55957	73.31	55.15	6.7	6000	2100	6.6	N.Z.
	1104	60257	49.97	77.79	6.0		34	5.4	
	1212	70057	43.85	54.77	6.6		190	6.0	
	1217	70057	49.73	78.13	6.1		35	5.4	
	1223	70057	43.83	54.85	6.6		240	6.0	E. Caspian Sea
1971	0322	43258	49.74	78.18	6.0		86	5.7	
	0323	65956	61.29	56.47	5.9	45	51	5.5	Urals
	0425	33258	49.82	78.09	6.4		140	5.9	
	0606	40257	49.98	77.77	5.5		39	5.5	
	0619	40358	50.01	77.74	5.4		36	5.4	

	0630	35657	49.97	79.05	5.9		25	5.2	
	0710	165959	64.17	55.18	5.1		27	5.2	Urals
	0919	110007	57.78	41.10			4	4.5	Urals
	0927	55955	73.39	55.10			770	6.5	N.Z.
	1009	60257	50.00	77.70			24	5.3	
	1021	66257	49.99	77.65			44	5.5	
	1022	50000	51.57	54.54			34	5.2	Urals
	1129	60257	49.76	78.13			34	5.4	
	1215	75259	49.98	77.90			3	4.9	
	1222	65956	47.87	48.22			210	6.0	N. Caspian Sea
	1230	62058	49.75	78.13			90	5.7	
1972	0210	50257	49.99	78.89	6.3		43	5.4	
	0310	45657	49.75	78.18	5.8		33	5.4	
	0328	42157	49.73	78.19	5.6		15	5.1	
	0411	60005	37.37	62.00	4.8		7		Turkman
	0607	12757	49.76	78.17	5.7		34	5.4	
	0706	10258	49.72	77.98	4.8		1	4.4	
	0709	65958	49.78	35.40	5.0		6	4.8	N. Black Sea
	0714	145949	50.00	46.40	3.6		0.2		N. Caspian Sea
	0816	31657	49.76	78.15	5.6		15	5.0	
	0820	25958	49.46	48.18	6.3		87	5.7	N. Caspian Sea
	0826	34657	49.99	77.78	5.8		35	5.3	
	0828	55957	73.34	55.08		1000	690	6.3	N.Z.
	0902	85658	49.96	77.73	5.3		7	4.9	
	0921	90001	52.13	51.99	5.2		21		N. Caspian Sea
	1003	85958	46.85	45.01	6.1		88	5.6	NW Caspian Sea
	1102	12658	49.91	78.84			350	6.1	
	1124	90008	52.78	51.07	5.1		11	4.5	Urals
	1124	95958	51.84	64.15	5.1		20	5.2	W. Kazakh
	1210	42658	49.85	78.18	6.0		70	5.6	
	1210	42708	50.11	78.81	6.7		620	6.0	
	1228	42713	51.70	79.20	4.9		3		
1973	0216	50258	49.83	78.23	5.5		48	5.5	
	0419	43258	50.01	79.72			27	5.4	
	0710	12658	49.78	78.06			28	5.2	
	0723	12258	49.99	78.85			420	6.1	
	0815	15958	42.71	67.41			28	5.3	Uzbekistan
	0828	25958	50.55	68.39			14	5.2	W. Kazakh
	0912	65954	73.30	55.16			2700	6.8	N.Z.
	0919	25957	45.63	67.85			11	5.1	W. Kazakh
	0927	65958	70.76	53.87			210	5.9	N.Z.
	0930	45957	51.61	54.58			22	5.2	Urals
	1026	42658	49.76	78.20			19	5.2	
	1026	55958	53.66	55.38			7	4.8	Urals
	1027	65957	70.78	54.18			3200	6.9	N.Z.
	1214	74657	50.04	79.01			150	5.8	
1974	0130	45658	49.89	77.99			2	4.9	
	0130	45702	49.83	78.08			23	5.2	
	0416	55302	49.99	78.82			3	4.9	
	0516	30257	49.74	78.15			23	5.2	
	0531	32657	49.95	78.84			140	5.9	
	0625	35658	49.89	78.11			2	4.7	
	0710	25657	49.79	78.14			16	5.2	
	0814	145958	68.91	75.90			45	5.4	N.Z.
	0829	95956	73.37	55.09			870	6.4	N.Z.
	0829	150000	67.23	62.12			20	5.0	Urals
	0913	30258	49.82	78.09			15	5.2	
	1016	63257	49.97	78.97			43	5.5	
	1102	45957	70.82	54.06			1600	6.4	N.Z.
	1207	55957	49.91	77.65			2	4.1	
	1216	62302	49.75	78.06			8	5.0	
	1216	64102	49.82	78.12			6	4.8	
	1227	54657	49.96	79.05			51	5.6	
1975	0220	53258	49.82	78.08			77	5.7	
	0311	54258	49.79	78.25			30	5.4	
	0427	53657	49.99	78.98			60	5.6	
	0608	32658	49.76	78.09			35	5.5	
	0807	35658	49.81	78.24			14	5.2	
	0823	85958	73.37	54.64			550	6.3	N.Z.
	0929	105958	69.59	90.40			6	4.8	W. Siberia
	1018	85956	70.84	53.69			1400	6.7	N.Z.
	1021	115957	73.35	55.08			700	6.6	N.Z.
	1029	44658	49.98	78.97			90	5.8	
	1213	45657	49.80	78.20			10	5.1	
	1225	51657	50.04	78.90			90	5.7	
1976	0115	44658	49.87	78.25			14	5.2	
	0421	50257	49.93	78.82			20	5.3	
	0704	25658	49.91	78.95			90	5.8	
	0723	23258	48.79	78.05			10	5.1	

REFERENCES

Aki, K. (1969), Analysis of the seismic coda of local earthquakes as scattered waves, J. Geophys. Res., 74, 615-631.

Aki, K. and B. Chouet (1975), Origin of coda waves: source, attenuation and scattering effects, J. Geophys. Res., 80, 3322-3342.

Antonova, L. V., F. F. Aptikayev, R. I. Kurochkina, I. L. Nersesov, A.V. Sitnikou, F. S. Tregub, L. D. Fedorskaya and V. I. Khalturin (1978), Experimental seismic investigations of the Earth's interior, Inst. of Phys. of the Earth, Nauka, Moscow, 155 p.

Baker, R. G. (1970), Determining magnitude from Lg, Bull. Seism. Soc. Am., 60, 1907-1920.

Barley, B. J., (1979), On the use of seismometer arrays to locate sources of higher mode Rayleigh waves, AWRE Report No. O 54178.

Bath, M. (1954), The elastic waves Lg and Rg along Euroasiatic paths, Arkiv. Geofys., 2, 295-324.

Bath, M. (1956), Some consequences of the existence of low velocity layers, Ann. Geofis., 9, 411-450.

Bath, M. (1956), Channel waves, J. Geophys. Res., 63, 583-587.

Bollinger, G. A. (1979), Attenuation of the Lg phase and the determination of m_b in the southeastern United States, Bull. Seism. Soc. Am., 69, 45-63.

Bolt, B. A., H. A. Doyle, and D. F. Sutton (1958), Seismic observations from the 1956 atomic explosions in Australia, Geophys. J.R. astr. Soc., 1, 135-145.

Bolt, B. A. (1976), Nuclear explosions and earthquakes - the parted veil, W. H. Freeman and Co, San Fransisco, 309 p.

Brune, J. and J.Dorman (1963), Seismic waves and earth structure in the Canadian Shield, Bull. Seism. Soc. Am., 53, 167-210.

Cheng, C. C. and B. J. Mitchell (1980), Crustal Q. structure in the United States from multi-mode surface waves, Semi-Annual Technical Report No. 3, Saint Louis University, St. Louis, MO.

Chinn, D. S., B. L. Isacks, and M. Barazangi (1980), High-frequency seismic wave propagation in western South America along the continental margin, in the Nazca Plate, and across the Altiplano, Preprint.

Chouet, B., K. Aki, and M. Tsujiura (1978), Regional variation of the scaling law of earthquake source spectra, Bull. Seism. Soc. Am., 68, 49-79.

Dahlman, O. and H. Israelson (1977), Monitoring underground nuclear explosions, Elsevier Scientific Publishing Co., Amsterdam, 440 p.

Dziewonski, A. M., S. Bloch, and M. Landisman (1969), A technique for the analysis of transient seismic signals, Bull. Seism. Soc. Am., 59, 427-444.

Gane, P. G., A. R. Atkins, J. P. F. Sellschop, and P. Seligmann (1956), Crustal structure in the Transvall, Bull. Seism. Soc. Am., 46, 293-316.

Gumper, F. and P. W. Pomeroy (1970), Siesmic wave velocities and earth structure on the African continent, Bull. Seism. Soc. Am., 60, 651-668.

Gupta, I. N., B. W. Barker, J. A. Burnetti, and Z. A. Der (1980), A study of regional phases from earthquakes and explosions in western Russia, Bull. Seism. Soc. Am., 70, 851-872.

Gutenberg, B. (1955), Channel waves in the Earth's crust, Geophys., 20, 283-294.

Herrin, E. and P. D. Minton (1960), The Velocity of Lg in the Southwestern United States and Mexico, Bull. Seism. Soc. Am., 50, 35-44.

Herrin, E. and J. Richmond (1960), On the Propagation of the Lg Phase, Bull. Seism. Soc. Am., 50, 197-210.

Herrin, E. (1961), On $\overline{P}$ and Lg, J. Geophys. Res., 66, 334-335.

Herrmann, R. B. (1980), Q estimates using the coda of local earthquakes, Bull. Seism. Soc. Am., 70, 447-468.

Herrmann, R. B. and O. W. Nuttli (1975), Ground-motion modelling at regional distances from earthquakes in a continental interior, I. Theory and observations, Earthq. engin. and struc. dyn., 4, 49-58.

Hodgson, J. H. (1953a), A seismic survey in the Canadian Shield I: Refraction studies based on rock-bursts at Kirtland Lake, Ont., Pub. Dominian Observatory, Ottawa, 16, 113-163.

Hodgson, J. H. (1953b), A seismic survey in the Canadian Shield II: Refraction studies based on timed blasts, Publ. Dominian Observatory, Ottawa, 16, 167-181.

Horner, R. B., A. E. Stevens, and H. S. Hasegawa (1973), The Bengough, Saskatchewan earthquake of July 26, 1972, Can. J. Earth Sci., 10, 1805-1821.

Isacks, B. L. and C. Stephens (1978), Conversion of Sn to Lg at a continental margin, Bull. Seism. Soc. Am., 65, 234-244.

Jeffreys, H. (1952), The times of P up to 30°, Mon. Notices of the R. astr. Soc., Geophys. Suppl., 6, 348-364.

Jeffreys, H. (1976), The Earth, Its Origin, History and Physical Constitution, Cambridge University Press, Cambridge, 6th Edition, 547 p.

Kadinsky-Cade, K. (1980), Short-period seismic wave propagation in the Middle East, Annual Technical Report No. 1, Cornell Univ., Ithaca, N.Y.

Knopoff, L., F. Schwab, and E. Kausel (1973), Interpretation of Lg, Geophys. J. R. astr. Soc., 33, 389-404.

Knopoff, L., F. Schwab, K. Nakanishi, and F. Chang (1974), Evaluation of Lg as discriminant among different continental crustal structures, Geophys. J. R. astr. Co., 39, 41-70.

Knopoff, L., R. G. Mitchel, E. G. Kausel, and F. Schwab (1979), A Search for the oceanic Lg phase, Geophys. J. R. astr. Soc., 56, 211-218.

Kovach, R. L. and D. L. Anderson (1964), Higher mode surface waves and their bearing on the structure of the Earth's mantle, Bull. Seism. Soc. Am., 54, 161-182.

Lehmann, I. (1953), On the short-period surface wave 'Lg' and crustal structure, Bul. d'Information, U.G.G.I., 2, 248-251.

McEvilly, T. V. (1964), Central U.S. crust - upper mantle structure from Love and Rayleigh wave phase velocity inversion, Bull. Seism. Soc. Am., 54, 1997-2015.

Mitchell, B. J. (1973a), Radiation and attenuation of Rayleigh waves from the southeastern Missouri earthquake of October 21, 1965, J. Geophys. Res., 78, 886-899.

Mitchell, B. J. (1973b), Surface-wave attenuation and crustal anelasticity in central North America, Bull. Seism. Soc. Am., 63, 1057-1071.

Mohorovičić, A. (1914), Das Beben vom 8 X 1909, Gerlands Beitrage zur Geophysik, 13, 217-240.

Nersesov, I. L. and T. G. Rautian (1964), Kinematics and dynamics of seismic waves to distances of 3500 km from the epicenter, Akad. Nauk SSSR, Trudy Inst. Fiziki Zemli, 32, 63-87.

Nuttli, O. W. (1973), Seismic wave attenuation and magnitude relations for eastern North America, J. Geophys. Res., 78, 876- .

Nuttli, O. W. (1978), A time-domain study of the attenuation of 10-Hz waves in the New Madrid seismic zone, Bull. Seism. Soc. Am., 68, 343-355.

Nuttli, O. W. (1980a), The excitation and attenuation of seismic crustal phases in Iran. Bull. Seism. Soc. Am., 70, 469-485.

Nuttli, O. W. (1980b), On the attenuation of Lg waves in western and central Asia and their use as a discriminant between earthquakes and explosions, Semi-Annual Technical Report No. 3, Saint Louis Univ., St. Louis, MO

Oliver, J. E., M. Ewing and F. Press (1955), Crustal structures of the Arctic regions from Lg phase, Geol. Soc. Am., 66, 1063-1074.

Oliver, J. and M. Ewing (1957), Higher modes of continental Rayleigh waves, Bull. Seism. Soc. Am., 47, 187-204.

Oliver, J. and M. Ewing (1958), Normal modes of continental surface waves, Bull. Seism. Soc. Am., 48, 33-49.

Panza, G. F., F. A. Schwab, and L. Knopoff (1972), Channel and crustal Rayleigh waves, Geophys. J. R. astr. Soc., 30, 273-280.

Panza, G. F. and G. Calcagnile (1975), Lg, Li and Rg from Rayleigh modes, Geophys. J. Roy. astr. Soc., 40, 475.

Piwinskii, A. J. and D. L. Springer (1978), Propagation of Lg waves across eastern Europe and Asia, Lawrence-Livermore Laboratory, U. Calif.

Pomeroy, P. W. and T. Nowak, (1978), An investigation of seismic wave propagation in western USSR, Semi-Annual Technical Report No. 2, Rondout Associates, Inc., Stone Ridge, NY.

Pomeroy, P. W. (1979), Regional seismic wave propagation, Semi-Annual Technical Report No. 3, Rondout Associates, Inc., Stone Ridge, NY.

Pomeroy, P. W. (1980), Regional seismic wave propagation, Semi-Annual Technical Report No. 4, Rondout Associates, Inc., Stone Ridge, NY.

Press, F. (1956), Velocity of Lg waves in Calif., Trans. Am. Geophys. Union, 37, 615-618.

Press, F. (1964), Seismic wave attenuation in the crust, J. Geophys. Res., 69, 4417-4418.

Press, F. and M. Ewing (1952), Two slow surface waves across North America, Bull. Seism. Soc. Am., 42, 219-228.

Rautian, T. G. and V. I. Khalturin (1978), The use of the coda for determination of the earthquake source mechanism, Bull. Seism. Soc. Am., 68, 923-948.

Richter, C. F. (1958), Elementary Seismology, W. H. Freeman and Co., San Fransisco, 768 p.

Romney, C., B. G. Brooks, R. H. Mansfield, D. S. Carder, J. N. Jordan, and D. W. Gordan (1962), Travel times and amplitudes of principal body phases recorded from GNOME, Bull. Seis. Soc. Am., 52, 1057-1074.

Ruzaikin, A. I., I. L. Nersesov, V. I. Khalturin, and P. Molnar (1977), Propagation of Lg and lateral variations in crustal structures in Asia, J. Geophys. Res., 82, 307-316.

Shishkevish, C. (1979), Propagation of Lg seismic waves in the Soviet Union, Rand Note, Santa Monica, Calif.

Singh, S. and R. B. Herrmann (1979), Q. Regionalization of western United States, Earthquake Notes, 50, No. 4, 27.

Springer, D. L. and R. L. Kinnaman (1971), Seismic source summary for U.S. underground nuclear explosions, 1961-1970, Bull. Seism. Soc. Am., 61, 1073-1098.

Springer, D. L. and R. L. Kinnaman (1975), Seismic-source summary for U.S. underground nuclear explosions, 1971-1973, Bull. Seism. Soc. Am., 65, 343-349.

Springer, D. L. and O. W. Nuttli (1980), Some characteristics of short-period seismic waves in southern Soviet Union, Semi-Annual Technical Report No. 3, Saint Louis Univ., St. Louis, MO.

Stauder, W. and G. Bollinger (1963), Pn velocity and other siesmic studies from the data of recent southeast Missouri earthquakes, Bull. Seism. Soc. Am., 53, 661-679.

Street, R. L. (1976), Scaling Northeastern United States/Southeastern Canadian Earthquakes by their Lg Waves, Bull. Seism. Soc. Am., 66, 1525.

Street, R. L., R. B. Herrmann and O. W. Nuttli (1975), Spectral characteristics of the Lg wave generated by central United States earthquakes, Geophys. J. Roy. astr. Soc., 41, 51-64.

Sutton, G. H., W. Mitrononvas, and P. W. Pomeroy (1967), Short-period seismic energy radiation patterns from underground nuclear explosions and small-magnitude earthquakes, Bull. Seism. Soc. Am., 57, 249-267.

Tsai, Y. B. and K. Aki (1969), Simultaneous determination of the seismic moment and attenuation of seismic surface waves, Bull. Seism. Soc. Am., 59, 275-287.